provide therapeutic benefits in humans even when given well after the ischemic episode.

Intriguingly, recent studies suggest that Zn^{2+} has multiple roles in this delayed selective neurodegeneration. In an *in vitro* slice model of acute ischemia, addition of either an extracellular Zn^{2+} chelator or a Ca^{2+} permeable AMPA channel blocker decreased both Zn^{2+} accumulation and consequent neuronal injury [21]. In an *in vivo* animal model, addition of an extracellular Zn^{2+} chelator either before or several days (but not several hours) after ischemia afforded neuroprotection. The early application of the chelator attenuated the downregulation of GluR2, suggesting a role for Zn^{2+} in signaling the increase in Ca^{2+} permeable AMPA channels. Whereas, late application of chelator, after Ca^{2+} permeable AMPA channel numbers had already risen, attenuated the late rise in intracellular Zn^{2+} associated with injury, suggesting that Ca^{2+} permeable AMPA channel dependent intracellular Zn^{2+} accumulation contributes to the delayed injury [49•].

Conclusions

Recent findings, reviewed above, suggest that increasing the number of Ca^{2+} permeable AMPA channels might contribute crucially to neurodegeneration in sporadic ALS and ischemia. The increase in Ca^{2+} permeable AMPA channels in these conditions could be achieved through different mechanisms: deficiencies in GluR2 mRNA editing in sporadic ALS or decreased levels of GluR2 mRNA in ischemia (Figure 2). In addition, basal levels of Ca^{2+} permeable AMPA channels appear to contribute to familial ALS associated with SOD1 mutations. Ca^{2+} permeable AMPA channels are probably also involved in other conditions including epilepsy and Alzheimer's disease, in which decreases in levels of GluR2 have been reported.

There are presently no selective Ca^{2+} permeable AMPA channel antagonists available for human trials or even for systemic administration in animals. Yet, the fact that Ca^{2+} permeable AMPA channels only constitute a minority of AMPA channels on most neurons makes them particularly attractive targets for therapeutics, as it could be possible to block much of the current through these channels without causing the degree of functional impairment that would accompany a comparable level of NMDA or total AMPA channel blockade. Furthermore, because an increase in Ca^{2+} permeable AMPA channel number might be integral to their pathological roles in certain conditions, in addition to the development of pharmacological antagonists, strategies for reducing their numbers or preventing their upregulation might also provide useful avenues for therapy.

Update

In a recent study [51••], Peng *et al.* report that forebrain ischemia in adult rats selectively disrupts Q/R site editing and the expression of GluR2 subunit mRNA in vulnerable neurons. The authors provide further evidence that the editing defect contributes to the consequent neurodegeneration of CA1 HPNs. Thus, these data suggest that alterations of GluR2 editing might not be unique to ALS, and that this mechanism might also contribute to delayed neurodegeneration after transient ischemia.

Acknowledgements

This work was supported by National Institutes of Health grant NS36548 (JH Weiss), a grant from the Muscular Dystrophy Association (JH Weiss), and a grant-in-aid for Scientific Research on Priority Areas from the Ministry of Education, Culture, Sports, Science and Technology of Japan 14017020, 15016030, 16015228 (S Kwak).

References and recommended reading

Papers of particular interest, published within the annual period of review, have been highlighted as:

- • of special interest
- •• of outstanding interest

1. Seeburg PH, Single F, Kuner T, Higuchi M, Sprengel R: **Genetic manipulation of key determinants of ion flow in glutamate receptor channels in the mouse.**. *Brain Res* 2001, **907**:233-243.

2. Kawahara Y, Kwak S: **Excitotoxicity and ALS, what is unique about the AMPA receptors expressed on spinal motor neurons?** *Amyotroph Lateral Scler Other Motor Neuron Disord* 2005, **6**:131-144.

3. Liu SQ, Cull-Candy SG: **Synaptic activity at calcium-permeable AMPA receptors induces a switch in receptor subtype.** *Nature* 2000, **405**:454-458.

4. • Gardner SM, Takamiya K, Xia J, Suh JG, Johnson R, Yu S, Huganir RL: **Calcium-permeable AMPA receptor plasticity is mediated by subunit-specific interactions with PICK1 and NSF.** *Neuron* 2005, **45**:903-915.
The authors demonstrate specific interactions between the GluR2 subunit of AMPA receptors and the cellular proteins involved in receptor trafficking. These interactions appear to underlie decreases in Ca^{2+} permeable AMPA channel numbers in response to physiological activation.

5. • Liu SJ, Cull-Candy SG: **Subunit interaction with PICK and GRIP controls Ca^{2+} permeability of AMPARs at cerebellar synapses.** *Nat Neurosci* 2005, **8**:768-775.
These authors (like those above) demonstrate specific interactions between the GluR2 subunit of AMPA receptors and the cellular proteins involved in receptor trafficking. These interactions appear to underlie decreases in Ca^{2+} permeable AMPA channel numbers in response to physiological activation.

6. Greger IH, Khatri L, Kong X, Ziff EB: **AMPA receptor tetramerization is mediated by Q/R editing.** *Neuron* 2003, **40**:763-774.

7. Greger IH, Khatri L, Ziff EB: **RNA editing at arg607 controls AMPA receptor exit from the endoplasmic reticulum.** *Neuron* 2002, **34**:759-772.

8. Beattie EC, Stellwagen D, Morishita W, Bresnahan JC, Ha BK, Von Zastrow M, Beattie MS, Malenka RC: **Control of synaptic strength by glial TNFalpha.** *Science* 2002, **295**:2282-2285.

9. • Ogoshi F, Yin HZ, Kuppumbatti Y, Song B, Amindari S, Weiss JH: **Tumor necrosis-factor-alpha (TNF-alpha) induces rapid insertion of Ca^{2+}-permeable alpha-amino-3-hydroxyl-5-methyl-4-isoxazole-propionate (AMPA)/kainate (Ca-A/K) channels in a subset of hippocampal pyramidal neurons.** *Exp Neurol* 2005, **193**:384-393.
The authors use Ca^{2+} imaging techniques to demonstrate membrane insertion of Ca^{2+} permeable AMPA channel in subpopulations of hippocampal pyramidal neurons in response to exposure to the solubule cytokine, TNF-alpha.

39

10. Stellwagen D, Beattie EC, Seo JY, Malenka RC: **Differential regulation of AMPA receptor and GABA receptor trafficking by tumor necrosis factor-alpha.** *J Neurosci* 2005, **25**:3219-3228.
• The authors report that TNF-alpha induces preferential exocytosis of GluR2-lacking AMPA receptors in hippocampal neurons.

11. Gorter JA, Petrozzino JJ, Aronica EM, Rosenbaum DM, Opitz T, Bennett MV, Connor JA, Zukin RS: **Global ischemia induces downregulation of Glur2 mRNA and increases AMPA receptor-mediated Ca^{2+} influx in hippocampal CA1 neurons of gerbil.** *J Neurosci* 1997, **17**:6179-6188.

12. Pellegrini-Giampietro DE, Gorter JA, Bennett MV, Zukin RS: **The GluR2 (GluR-B) hypothesis: Ca^{2+}-permeable AMPA receptors in neurological disorders.** *Trends Neurosci* 1997, **20**:464-470.

13. Kawahara Y, Ito K, Sun H, Aizawa H, Kanazawa I, Kwak S:
•• **Glutamate receptors: RNA editing and death of motor neurons.** *Nature* 2004, **427**:801.
The authors demonstrate that in sporadic ALS, MNs, but not Purkinje cells, have abundant GluR2 mRNA that is unedited at the Q/R site. The specificity of this finding to MNs and the demonstrated ability of the activation of Ca^{2+} permeable AMPA channels to injure neurons suggest that this molecular change might be tightly linked to the etiology of MN death in sporadic ALS.

14. Kwak S, Kawahara Y: **Deficient RNA editing of GluR2 and
• neuronal death in amyotropic lateral sclerosis.** *J Mol Med* 2005, **83**:110-120.
The authors review the AMPA receptor-mediated neuronal death in ALS, and discuss mechanisms that might underlie the underediting of GluR2 mRNA in MNs.

15. Takuma H, Kwak S, Yoshizawa T, Kanazawa I: **Reduction of GluR2 RNA editing, a molecular change that increases calcium influx through AMPA receptors, selective in the spinal ventral gray of patients with amyotrophic lateral sclerosis.** *Ann Neurol* 1999, **46**:806-815.

16. Hong SJ, Dawson TM, Dawson VL: **Nuclear and mitochondrial conversations in cell death: PARP-1 and AIF signaling.** *Trends Pharmacol Sci* 2004, **25**:259-264.

17. Koh JY, Suh SW, Gwag BJ, He YY, Hsu CY, Choi DW: **The role of zinc in selective neuronal death after transient global cerebral ischemia.** *Science* 1996, **272**:1013-1016.

18. Lee JY, Kim JH, Palmiter RD, Koh JY: **Zinc released from metallothionein-iii may contribute to hippocampal CA1 and thalamic neuronal death following acute brain injury.** *Exp Neurol* 2003, **184**:337-347.

19. Jia Y, Jeng JM, Sensi SL, Weiss JH: **Zn^{2+} currents are mediated by calcium-permeable AMPA/kainate channels in cultured murine hippocampal neurones.** *J Physiol* 2002, **543**:35-48.

20. Sensi SL, Yin HZ, Carriedo SG, Rao SS, Weiss JH: **Preferential Zn^{2+} influx through Ca^{2+}-permeable AMPA/kainate channels triggers prolonged mitochondrial superoxide production.** *Proc Natl Acad Sci USA* 1999, **96**:2414-2419.

21. Yin HZ, Sensi SL, Ogoshi F, Weiss JH: **Blockade of Ca^{2+}-permeable AMPA/kainate channels decreases oxygen-glucose deprivation-induced Zn^{2+} accumulation and neuronal loss in hippocampal pyramidal neurons.** *J Neurosci* 2002, **22**:1273-1279.

22. Kim YH, Koh JY: **The role of NADPH oxidase and neuronal nitric oxide synthase in zinc-induced poly(ADP-ribose) polymerase activation and cell death in cortical culture.** *Exp Neurol* 2002, **177**:407-418.

23. Jiang D, Sullivan PG, Sensi SL, Steward O, Weiss JH: **Zn^{2+} induces permeability transition pore opening and release of pro-apoptotic peptides from neuronal mitochondria.** *J Biol Chem* 2001, **276**:47524-47529.

24. Sensi SL, Ton-That D, Sullivan PG, Jonas EA, Gee KR, Kaczmarek LK, Weiss JH: **Modulation of mitochondrial function by endogenous Zn^{2+} pools.** *Proc Natl Acad Sci USA* 2003, **100**:6157-6162.

25. Bossy-Wetzel E, Talantova MV, Lee WD, Scholzke MN, Harrop A, Mathews E, Gotz T, Han J, Ellisman MH, Perkins GA *et al.*: **Crosstalk between nitric oxide and zinc pathways to neuronal cell death involving mitochondrial dysfunction and p38-activated K^+ channels.** *Neuron* 2004, **41**:351-365.

26. Rothstein JD, Martin LJ, Kuncl RW: **Decreased glutamate transporter by the brain and spinal cord in amyotrophic lateral sclerosis.** *N Engl J Med* 1992, **326**:1464-1468.

27. Carriedo SG, Yin HZ, Weiss JH: **Motor neurons are selectively vulnerable to AMPA/kainate receptor-mediated injury in vitro.** *J Neurosci* 1996, **16**:4069-4079.

28. Rothstein JD, Jin L, Dykes-Hoberg M, Kuncl RW: **Chronic inhibition of glutamate uptake produces a model of slow neurotoxicity.** *Proc Natl Acad Sci USA* 1993, **90**:6591-6595.

29. Van Den Bosch L, Vandenberghe W, Klaassen H, Van Houtte E, Robberecht W: **Ca^{2+}-permeable AMPA receptors and selective vulnerability of motor neurons.** *J Neurol Sci* 2000, **180**:29-34.

30. Vandenberghe W, Robberecht W, Brorson JR: **AMPA receptor calcium permeability, GluR2 expression, and selective motoneuron vulnerability.** *J Neurosci* 2000, **20**:123-132.

31. Kawahara Y, Kwak S, Sun H, Ito K, Hashida H, Aizawa H, Jeong S-Y, Kanazawa I: **Human spinal motoneurons express low relative abundance of GluR2 mRNA: An implication for excitotoxicity in ALS.** *J Neurochem* 2003, **85**:680-689.

32. Sun H, Kawahara Y, Ito K, Kanazawa I, Kwak S: **Expression profile of AMPA receptor subunit mRNA in single adult rat brain and spinal cord neurons in situ.** *Neurosci Res* 2005, **52**:228-234.

33. Kawahara Y, Sun H, Ito K, Hideyama T, Aoki M, Sobue G, Tsuji S,
• Kwak S: **Underediting of GluR2 mRNA, a neuronal death inducing molecular change in sporadic ALS, does not occur in motor neurons in ALS1 or SBMA.** *Neurosci Res* 2006, **54**:11-14.
Although animals carrying mutated human SOD1 are the most widely used models for ALS, this paper reports that in these animals, and in humans with SBMA, the GluR2 editing defects do not occur. This suggests that differing molecular mechanisms underlie sporadic and familial forms of ALS.

34. Nagano I, Murakami T, Shiote M, Abe K, Itoyama Y: **Ventral root avulsion leads to downregulation of GluR2 subunit in spinal motoneurons in adult rats.** *Neuroscience* 2003, **117**:139-146.

35. Darman J, Backovic S, Dike S, Maragakis NJ, Krishnan C,
• Rothstein JD, Irani DN, Kerr DA: **Viral-induced spinal motor neuron death is non-cell-autonomous and involves glutamate excitotoxicity.** *J Neurosci* 2004, **24**:7566-7575.
The authors report that Ca^{2+} permeable AMPA channel blockers offer protection against MN death caused by a viral infection, supporting the contention that Ca^{2+} permeable AMPA channel activation contributes to MN degeneration in diverse conditions.

36. Kuner R, Groom AJ, Bresink I, Kornau HC, Stefovska V, Muller G,
•• Hartmann B, Tschauner K, Waibel S, Ludolph AC *et al.*: **Late-onset motoneuron disease caused by a functionally modified AMPA receptor subunit.** *Proc Natl Acad Sci USA* 2005, **102**:5826-5831.
In this study, mice transgenic for GluR-B(N), an artificial gene resulting in increased Ca^{2+} permeability of AMPA channels, developed slow onset of MN loss, indicating that increasing Ca^{2+} permeable AMPA channel numbers (as probably occurs from underediting of GluR2) does result in preferential MN injury. Additional presence of mutant SOD1 in these animals accelerated disease progression, indicating synergism between Ca^{2+} permeable AMPA channel activation and mutant SOD1 in mediating MN degeneration.

37. Van Damme P, Braeken D, Callewaert G, Robberecht W, Van Den
• Bosch L: **GluR2 deficiency accelerates motor neuron degeneration in a mouse model of amyotrophic lateral sclerosis.** *J Neuropathol Exp Neurol* 2005, **64**:605-612.
The authors report that deletion of the GluR2 subunit caused increased Ca^{2+} permeable AMPA channel number in MNs and accelerated MN loss in SOD1 mutant mice, again indicating synergistic effects of Ca^{2+} permeable AMPA channel activation and mutant SOD1.

38. Tateno M, Sadakata H, Tanaka M, Itohara S, Shin RM, Miura M,
• Masuda M, Aosaki T, Urushitani M, Misawa H *et al.*: **Calcium-permeable AMPA receptors promote misfolding of mutant SOD1 protein and development of amyotrophic lateral**

40

sclerosis in a transgenic mouse model. *Hum Mol Genet* 2004, **13**:2183-2196.
Taking the opposite approach to the two papers above [36••,37•], these authors find that decreasing the number of Ca^{2+} permeable AMPA channels in MNs (by targeted GluR2 overexpression) delays the MN loss and prolongs survival in SOD1 mutant mice. This provides further evidence for a role of Ca^{2+} permeable AMPA channel activation in this familial form of ALS.

39. Lips MB, Keller BU: **Endogenous calcium buffering in motoneurones of the nucleus hypoglossus from mouse.** *J Physiol* 1998, **511**:105-117.

40. Carriedo SG, Sensi SL, Yin HZ, Weiss JH: **AMPA exposures induce mitochondrial Ca^{2+} overload and ROS generation in spinal motor neurons in vitro.** *J Neurosci* 2000, **20**:240-250.

41. Rao SD, Yin HZ, Weiss JH: **Disruption of glial glutamate transport by reactive oxygen species produced in motor neurons.** *J Neurosci* 2003, **23**:2627-2633.

42. • Rao SD, Weiss JH: **Excitotoxic and oxidative cross-talk between motor neurons and glia in ALS pathogenesis.** *Trends Neurosci* 2004, **27**:17-23.
The authors consider the evidence that ROS produced in MNs might account for disruption of astrocytic glutamate transport, and discuss how this mechanism could underlie a feed-forward model of ALS progression and provide a basis for observations that MN loss in ALS is 'non-cell-autonomous'.

43. Lerma J, Morales M, Ibarz JM, Somohano F: **Rectification properties and Ca^{2+} permeability of glutamate receptor channels in hippocampal cells.** *Eur J Neurosci* 1994, **6**:1080-1088.

44. Ogoshi F, Weiss JH: **Heterogeneity of Ca^{2+}-permeable AMPA/kainate channel expression in hippocampal pyramidal neurons: fluorescence imaging and immunocytochemical assessment.** *J Neurosci* 2003, **23**:10521-10530.

45. Yin HZ, Sensi SL, Carriedo SG, Weiss JH: **Dendritic localization of Ca^{2+}-permeable AMPA/kainate channels in hippocampal pyramidal neurons.** *J Comp Neurol* 1999, **409**:250-260.

46. Anzai T, Tsuzuki K, Yamada N, Hayashi T, Iwakuma M, Inada K, Kameyama K, Hoka S, Saji M: **Overexpression of Ca^{2+}-permeable AMPA receptor promotes delayed cell death of hippocampal CA1 neurons following transient forebrain ischemia.** *Neurosci Res* 2003, **46**:41-51.

47. • Liu S, Lau L, Wei J, Zhu D, Zou S, Sun HS, Fu Y, Liu F, Lu Y: **Expression of Ca(2+)-permeable AMPA receptor channels primes cell death in transient forebrain ischemia.** *Neuron* 2004, **43**:43-55.
These authors varied Ca^{2+} permeable AMPA channel levels in both directions, and found that decreasing their number (by overexpression of edited GluR2) attenuated ischemic injury in the CA1 subfield, whereas increasing Ca^{2+} permeable AMPA channels (by overexpression of unedited GluR2) resulted in new ischemic damage to granule neurons.

48. •• Noh KM, Yokota H, Mashiko T, Castillo PE, Zukin RS, Bennett MV: **Blockade of calcium-permeable AMPA receptors protects hippocampal neurons against global ischemia-induced death.** *Proc Natl Acad Sci USA* 2005, **102**:12230-12235.
The authors provide electrophysiological evidence for a substantial rise in the number of Ca^{2+} permeable AMPA channels on CA1 pyramidal neurons at 42 h after transient global ischemia. In addition, they find that addition of a Ca^{2+} permeable AMPA channel blocker between 9 and 40 h after the ischemia was partially protective and markedly reduced the rise in Zn^{2+} levels observed to proceed neuronal death.

49. • Calderone A, Jover T, Mashiko T, Noh KM, Tanaka H, Bennett MV, Zukin RS: **Late calcium EDTA rescues hippocampal CA1 neurons from global ischemia-induced death.** *J Neurosci* 2004, **24**:9903-9913.
These authors report that addition of the Zn^{2+} chelator, Ca- EDTA, can decrease CA1 neuronal degeneration in distinct ways depending upon the time of delivery. Early Ca-EDTA (before ischemia) prevented the GluR2 downregulation, cytochrome C release and other indices of mitochondrial disruption. By contrast, late Ca-EDTA (48–60 h after ischemia), when GluR2 is already downregulated, attenuated the late Zn^{2+} rises observed to precede cell death. The findings of this and the previous paper [48••] support the therapeutic efficacy of Ca^{2+} permeable AMPA channel blockade or Zn^{2+} chelation when delivered long after an ischemic insult.

50. Nishimoto Y, Hideyama T, Kawahar Y, Kwak S: **Reduction of RNA editing of an AMPA receptor subunit GluR2 and death of motor neurons in ALS (in Japanese).** *Clinical Neuroscience* 2006, **24**:222-225.

51. •• Peng PL, Zhong X, Tu W, Soundarapandian MM, Molner P, Zhu D, Lau L, Liu S, Liu F, Lu Y: **ADAR2-dependent RNA editing of AMPA receptor subunit GluR2 determines vulnerability of neurons in forebrain ischemia.** *Neuron* 2006, **49**:719-733.
The authors use single cell PCR to show that forebrain ischemia in adult rats selectively disrupts Q/R site editing through downregulation of the editing enzyme adar2. They also provide evidence that this editing defect contributes to the delayed selective degeneration of CA1 hippocampal pyramidal neurons.

Aging of Complex Heart Rate Dynamics

Zbigniew R. Struzik, Junichiro Hayano, Rika Soma, Shin Kwak, and Yoshiharu Yamamoto

Abstract—**We reveal unexpected origins of age induced departure from $1/f$-type temporal scaling in healthy human heart rate. Contrary to the widely established view, we provide evidence that age induced dynamical imbalance in the autonomic control is not due to the emergent functional dominance of the sympathetic nervous system (SNS), but due to emerging (age dependent) relative dynamic dominance of the parasympathetic nervous system function. In particular, we demonstrate that the age induced alterations of healthy heart rate dynamics asymptotically resemble those in so-called primary autonomic failure with neurogenic SNS dysfunction and in other neurodegenerative disorders, including Parkinson's disease even without known autonomic abnormalities. Based upon this, we propose a novel picture of "autonomic aging," characterized by an insufficiency of the SNS function to cope dynamically with various environmental stimuli.**

Index Terms—**Aging, autonomic nervous system, heart rate variability, multifractals, $1/f$ noise.**

I. Introduction

HEALTHY human heart rate has been known to display fairly complex dynamics, exhibiting long-range temporal correlations [1], [2], non-Gaussianity of the increment's probability density function [1], as well as multifractality [3], [4], all reminiscent of real-world complex signals in physics, e.g., fluid turbulence [5], [6] and critical phenomena [7]–[9]. Physiologically, the origin of the complex dynamics of heart rate has been attributed to an intricate balance between the two branches of the autonomic nervous system: the parasympathetic (PNS) and the sympathetic (SNS) nervous systems, respectively, decreasing and increasing heart rate [1], [2], [4], [10]. In fact, Struzik *et al.* [11] recently reported that the disease-induced relative dysfunction of either PNS or SNS results in more correlated heart rate dynamics, but only the PNS dysfunction leads to reduced multifractality.

Although it has been conjectured that there is both a functional and a structural loss of complexity due to aging [12], the effect of aging on complex heart rate dynamics in humans has not been fully elucidated. Heart rate responses to selective and/or combined autonomic blockades of PNS and SNS [13], [14], plasma concentration of the sympathetic neurotransmitters [15], and the magnitude of respiratory modulation of heart rate [16]–[19], one of the robust indicators of PNS function [20], [21], all exhibit changes compatible with the increased SNS and decreased PNS function with aging. This might lead to the conjecture that aging is associated with increased long-range correlation, as demonstrated previously [22]–[24], and with decreased multifractality, as have been observed in congestive heart failure (CHF) [3] with relative SNS augmentation [25], [26] and PNS dysfunction [25], [27].

Here, however, we present an unexpected observation regarding the complex dynamical interaction between two branches of the autonomic control system, namely that normative aging is associated with increased long-range correlation *but with preserved multifractality*. The direction of change is consistent with that observed in patients suffering from central SNS dysfunction due to primary autonomic failure (PAF) [28], [29], not with the direction observed in CHF. We believe that our findings will give rise to a novel picture of "autonomic aging" as a progressive loss of the SNS function and its ability to cope dynamically with various environmental stimuli.

II. Data

We analyze 115 healthy subjects (26 women and 89 men; ages 16–84 years) without any known disease affecting autonomic control of heart rate. They underwent ambulatory monitoring during normal daily life, and the long-term heart rate data were measured as sequential heart interbeat intervals. The total number of whole-day data sets is 181, as most of the subjects were examined for two consecutive days, with each data set containing on average 10^5 heartbeats. For each subject, on an individual basis, we have excluded the possibility of any bias in the results caused by two consequtive days of heart rate recording ($p = 0.54$ by paired t-test for the individual daily Hurst exponent).

Details of the recruitment of the subjects, screening for medical problems, protocols and the data collection and preprocessing are described in [30]. We analyzed both whole-day data containing periods of sleep and waking and daytime data, with essentially identical results. In this paper, we present only daytime results.

As a reference, we describe the results previously obtained for 24-hour ambulatory heart rate dynamics of 10 PAF patients (3 women and 7 men) aged 54–77 years (mean age 64.8) [28], containing on average 10^5 heartbeats [11]. The selection of the subjects and the collection procedures for this data are described in [11]. PAF is clinically characterized as autonomic dysfunction, including orthostatic hypotension, impotence, bladder and bowel dysfunction and sweating defects, which primarily result from progressive neuronal degeneration of unknown cause. The main pathological finding related to autonomic dysfunction in PAF is severe loss of preganglionic and/or postganglionic sympathetic

Manuscript received October 20, 2004; revised May 8, 2005. This work was supported in part by the Japan Science and Technology Agency. *Asterisk indicates corresponding author.*

*Z. R. Struzik is with the Educational Physiology Laboratory, Graduate School of Education, The University of Tokyo, 7-3-1 Hongo, Bunkyo-ku, Tokyo 113-0033, and PRESTO, Japan Science and Technology Agency, Kawaguchi, Saitama 332-0012, Japan (e-mail: Zbigniew.Struzik@p.u-tokyo.ac.jp).

J. Hayano is with the Core Laboratory, Nagoya City University Graduate School of Medical Sciences, Nagoya 467-8601, Japan.

R. Soma and Y. Yamamoto are with the Educational Physiology Laboratory, Graduate School of Education, The University of Tokyo, Tokyo 113-0033, Japan, and PRESTO, Japan Science and Technology Agency, Kawaguchi, Saitama 332-0012, Japan.

S. Kwak is with the Department of Neurology, Graduate School of Medicine, The University of Tokyo, Tokyo 113-0033, Japan.

Digital Object Identifier 10.1109/TBME.2005.859801

0018-9294/$20.00 © 2006 IEEE

neurons [29], and it is, thus, considered that this group serves as an example of relative and *neurogenic* SNS dysfunction.

Further, we also include the results for 12 CHF subjects (3 women and 9 men, with ages between 22 and 71, average 60.8 years) [11]. For details of the data acquisition and pre-processing see [3].

Finally, in a combined group with PAF patients, we also use additional 24-hour ambulatory heart rate data obtained from 5 patients, including four Parkinson's disease (PD) patients and one patient (74 years, male) showing "pure akinesia," one of the clinical features of Parkinsomism, without known autonomic abnormalities, containing on average 10^5 heartbeats. All the PD patients had bradykinesia and rigidity-predominant PD with apparent L-dopa responsiveness. There were 4 men and 1 woman, with a mean age of 67.2 years (range 56 to 74 years) and the mean disease duration was 11.2 years (range 3 to 24 years). All the patients received regular antiparkinsonian medication before and during the test days. The data, 24-hour heartbeat intervals of the PD patients during a hospital stay, were collected using a portable ambulatory monitor [31].

III. Analysis Methods

A. DFA Analysis of Aging

To evaluate the degree of long-range temporal correlation, the scaling exponent (the Hurst exponent H) has been calculated by using (first-order) detrended fluctuation analysis (DFA) [32], [33], as described below.

We have (arbitrarily) selected a number of age groups to assess mean scaling per group. The groups chosen are less than forty (40-), forty to sixty (40–60), sixty to eighty (60–80), and above eighty (80+) years. We have analyzed the scaling behavior of the mean quantity (group mean) $\bar{M}_{\mathrm{DFA}}(s) = L^{-1}\sum_{l=1}^{L}\log_{10}(D_{\mathrm{DFA}}^{(l)}(s))$, where l indexes time series in the group. For each scale/resolution s as measured by the DFA window size, and for each integrated, normalized heartbeat interval time series $\{F_i^{(l)} = T_l^{-1}\sum_{j=1}^{i} f_j^{(l)}\}_{(i=1,\ldots,N_l),(l=1,\ldots,L)}$, $D_{\mathrm{DFA}}^{(l)}(s)$ (total scalewise detrended fluctuation) has been calculated

$$D_{\mathrm{DFA}}^{(l)}(s) = s^{-1}\sqrt{\frac{1}{K^{(l)}(s)}\sum_{k=1}^{K^{(l)}(s)}\left(F_k^{(l)} - P_k(s)\right)^2}.$$

$P_k(s)$ denotes the local least-squares linear fit in each DFA window k, and $K^{(l)}(s)$ is the number of windows per scale s. Integration of the input heartbeat intervals is performed according to standard DFA practice, and the norm used is the elapsed time $T_l = \sum_{i=1}^{N_l} f_i^{(l)}$. The normalization applied allows us to compute group averages of records of different duration, and to compare the mean absolute levels of variability per resolution s; for each resolution s, the quantity $\bar{M}_{\mathrm{DFA}}(s)$ measures the (logarithmic) scalewise mean of the normalized DFA (the sum of the logarithm of detrended fluctuations for each group of time series at this resolution). The Hurst exponent was computed from the log-log fit to the group averaged DFA values over the selected range of scales (20–4000 beats).

B. Multifractal Analysis of Aging

We have also tested the multifractal properties of the data using the wavelet-based multifractal methodology [34]. We apply the second derivative of the Gaussian to the data as the mother wavelet before calculating the partition function $Z_q(s)$, defined as the sum of the qth powers of the local maxima of the modulus of the wavelet transform coefficients at scale s. The power law scaling of $Z_q(s)$ for $13 < s < 850$ then yields the scaling exponents $\tau(q)$ (the multifractal spectrum). The multifractal spectrum is related to the singularity spectrum $D(h)$, where $D(h_o)$ is the fractal dimension of the subset of the original time series characterized by a *local* Hurst exponent $h = h_o$ [35], through a Legendre transform $D(h) = qh - \tau(q)$ with $h = d\tau(q)/dq$.

In order to provide group mean values, we have analyzed the scaling behavior of the mean quantity $\bar{M}_{\mathrm{WTMM}}(q,s) = L^{-1}\sum_{l=1}^{L}\log_{10}(\mathcal{Z}_{\mathrm{WTMM}}^{(l)}(q,s))$, where l indexes time series in the group. For each scale/resolution s as measured by the wavelet size, and for each integrated, normalized heartbeat interval time series $\{F_i^{(l)} = T_l^{-1}\sum_{j=1}^{i} f_j^{(l)}\}_{(i=1,\ldots,N_l),(l=1,\ldots,L)}$, $\mathcal{Z}_{\mathrm{WTMM}}^{(l)}(q,s)$ (the multifractal partition function) has been calculated

$$\mathcal{Z}_{\mathrm{WTMM}}^{(l)}(q,s) = \sum_{k=1}^{K^{(l)}(s)}\left(\mathcal{WT}_{\omega_k}(s)(F^{(l)})\right)^q.$$

$\mathcal{WT}_{\omega_k}(s)(F^{(l)})$ denotes the kth maximum of the modulus of the wavelet transform $\mathcal{WT}$ of the time series $F^{(l)}$, and $K^{(l)}(s)$ is the number of maxima per scale s. As in the case of the DFA analysis above, the norm used is the elapsed time $T_l = \sum_{i=1}^{N_l} f_i^{(l)}$.

Similarly to the case of the mean DFA analysis, the normalization applied allows us to compute group averages of records of different duration; for each resolution s, the quantity $\bar{M}_{\mathrm{WTMM}}(s)$ measures the (logarithmic) scalewise mean of the normalized partition function $\mathcal{Z}(q,s)$ parameterized with the moment q. $\tau(q)$ is, thus, obtained by linear fit to the mean quantity $\bar{M}_{\mathrm{WTMM}}(s)$ versus $\log(s)$. The Legendre transform is implemented by a linear fit in the $\tau(q)$ domain; from 100 samples of q in the range $-15 \le q \le 15$, one-quarter, i.e., 25, of the available points is used to obtain $h(q)$ as a function of q, as the best local linear fit to $\tau(q)$, centered at q. $D(h(q))$ is then calculated in a straightforward way. Note that only the useful range $-6 \le q \le 6$ is shown in the $\tau(q)$ plots and used for $D(h)$ plots.

IV. Results

In Fig. 1, we show the dependence of the estimated scaling exponent H for the range of resolutions used (16–4000 beats) on age for each healthy subject. A steady increase in H can be observed, consistent with previously reported findings using Fourier methods of scaling exponent estimation [19], [24] and DFA for age groups of young and old [22]–[24].

In Fig. 2, we show the scaling behavior of the $\log_{10}(\bar{D}_{\mathrm{DFA}}(s))$ versus $\log_{10}(s)$ for the different age groups. We identify a systematic tendency of the decrease in scalewise variability with aging for the healthy group. This holds for the entire compared resolution range of 4–4000 beats as measured by the DFA window size s.

Although the extremely low PAF variability is not reached by healthy adults even in the group over the age of 80 years old, the levels of variability at the highest resolutions (and lowest

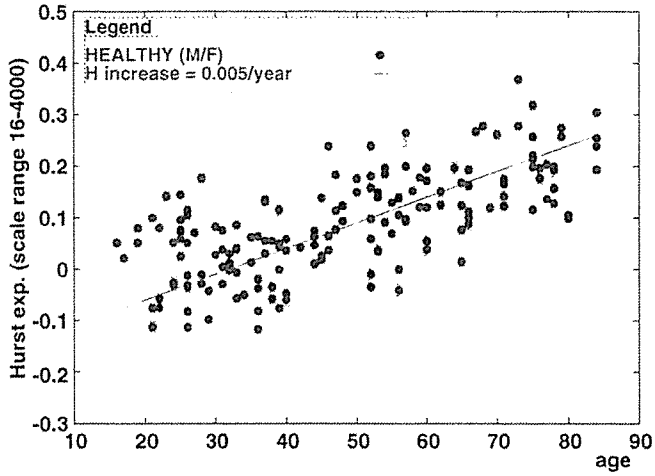

Fig. 1. Typical age-related departure from $1/f$ scaling for healthy heart rate showing a steady increase. First-order DFA, i.e., linear trend removal [32], is used for the estimation of the Hurst exponent H from the daytime records of heartbeat intervals of healthy subjects.

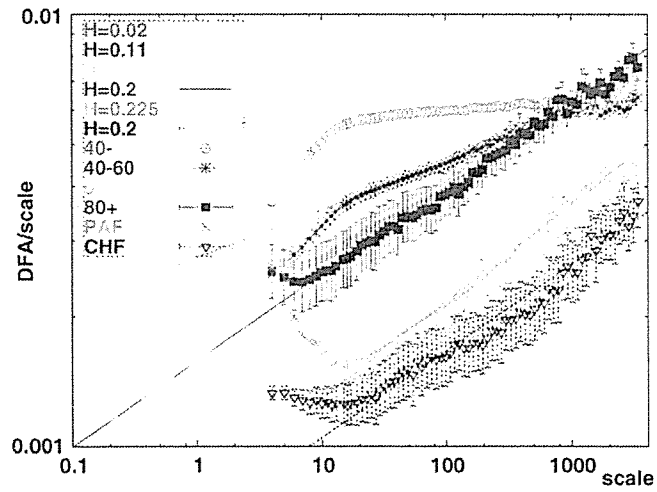

Fig. 2. Scale dependency of the mean detrended fluctuation $\bar{D}_{\mathrm{DFA}}(s)$ for four age groups of healthy subjects and for the PAF patients. Detrended fluctuations have been calculated with first-order DFA, i.e., linear trend removal [32]. The vertical bars represent the standard deviations of the group means.

beat numbers) remain relatively well conserved for all ages, reflecting the preservation of high-frequency fluctuations of heart rate, indicative of the intact PNS function [20], [21], in the elder groups as well as in the PAF patients. This contrasts with the reported [11] considerable decrease in CHF variability at all resolutions, including variability decrease the highest resolutions (presumably due to the decreased PNS function).

Consistent with the results depicted in Fig. 1, we confirm the age-related systematic (and substantial) increase in the Hurst exponent H of the analyzed age groups from $1/f$ corresponding with $H = 0.0$ to $H > 0.2$ for advanced age, i.e., toward the value which is both observed in the relative PNS dysfunction by CHF and in the PAF induced relative SNS dysfunction [11] (Fig. 2). This effect has been observed for the entire range of resolutions with almost consistent scaling, which for all groups analyzed stretches from about 20 beats up to the maximum resolution used of 4000 beats (DFA window size).

From the above established facts, it would be difficult to determine which branch of the autonomic nervous system suffers due to aging. Affecting the PSN/SNS balance by both the relative and neurogenic SNS dysfunction by PAF and by the relative PNS dysfunction by CHF results in a strong decrease in scale-wise variability and an increase of the scaling exponent H. The only indicator of the intact PNS function in the above is the relatively well-conserved variability at the highest resolutions, i.e., at the lowest beat numbers, as also suggested in a previous study [16].

Therefore, in order to provide further evidence for the preserved PNS function with aging, we have also tested the multifractal properties of the data, shown to be observed only with the functional PNS [11], using the wavelet-based multifractal methodology [34].

We obtain a comparable, wide singularity spectra $D(h)$ for all the healthy age groups, indicative of preserved multifractality with advancing age (Fig. 3). While multifractality has been shown to be nearly lost in the case of CHF patients [3], it has recently been shown to be maintained in the case of PAF patients [11]. Thus, it seems that autonomic aging mimics PAF, but not CHF with the SNS predominance, and we have obtained surprising evidence that the age induced dynamical imbalance in the autonomic control may not reflect the relative increase in SNS function but rather be related to a dynamical and *relative* decrease of it.

V. Emerging Picture of Autonomic Aging

At present, the mechanism for this observation is unknown, but two possibilities exist. First, the elderly are known to show a decrease in vasoconstrictive responses to sympathetic stimulation [36], which would lead to functionally similar effects to PAF with neurogenic SNS dysfunction. Second, age-related degeneration in the brain stem dopaminergic, as well as noradrenergic neurons [37], and the resultant direct and/or indirect (through the limbic system) effects on the medullary cardiovascular centers may be responsible for the similarity in the heart rate dynamics of the elderly to those of PAF patients, and possibly of PD patients even without autonomic failure. Aging is indeed known to be associated with manifestations of signs of Parkinsomism [38], of which neuronal degeneration in the dopaminergic substantia nigra and the noradrenergic locus coeruleus is the main neuropathology [39].

To confirm the second possibility, we created a combined group of "simulated autonomic aging" by mixing the data from the PAF group with the heart rate data obtained from 5 patients, including four PD patients and one patient (74 years, male) showing "pure akinesia," one of the clinical features of Parkinsomism, without known autonomic abnormalities.

We verify that mixing PD patients without known autonomic abnormality with PAF patients also results in a consistent increase in the DFA slope greater than that of the oldest age group of over eighty years of age, see Fig. 4. As shown in Fig. 5, this new "simulated autonomic aging" group shows a systematic increase in the DFA slope, even when compared with the age-matched healthy controls, with preserved multi-fractality (Fig. 6). This suggests that these neurodegenerative diseases have a similar effect on heart rate dynamics, i.e., increased Hurst exponent and preserved multifractality, to that of normative aging. It is of note that both PAF [29] and PD [40] are known to have sympathetic dysfunction, consistent with a scenario

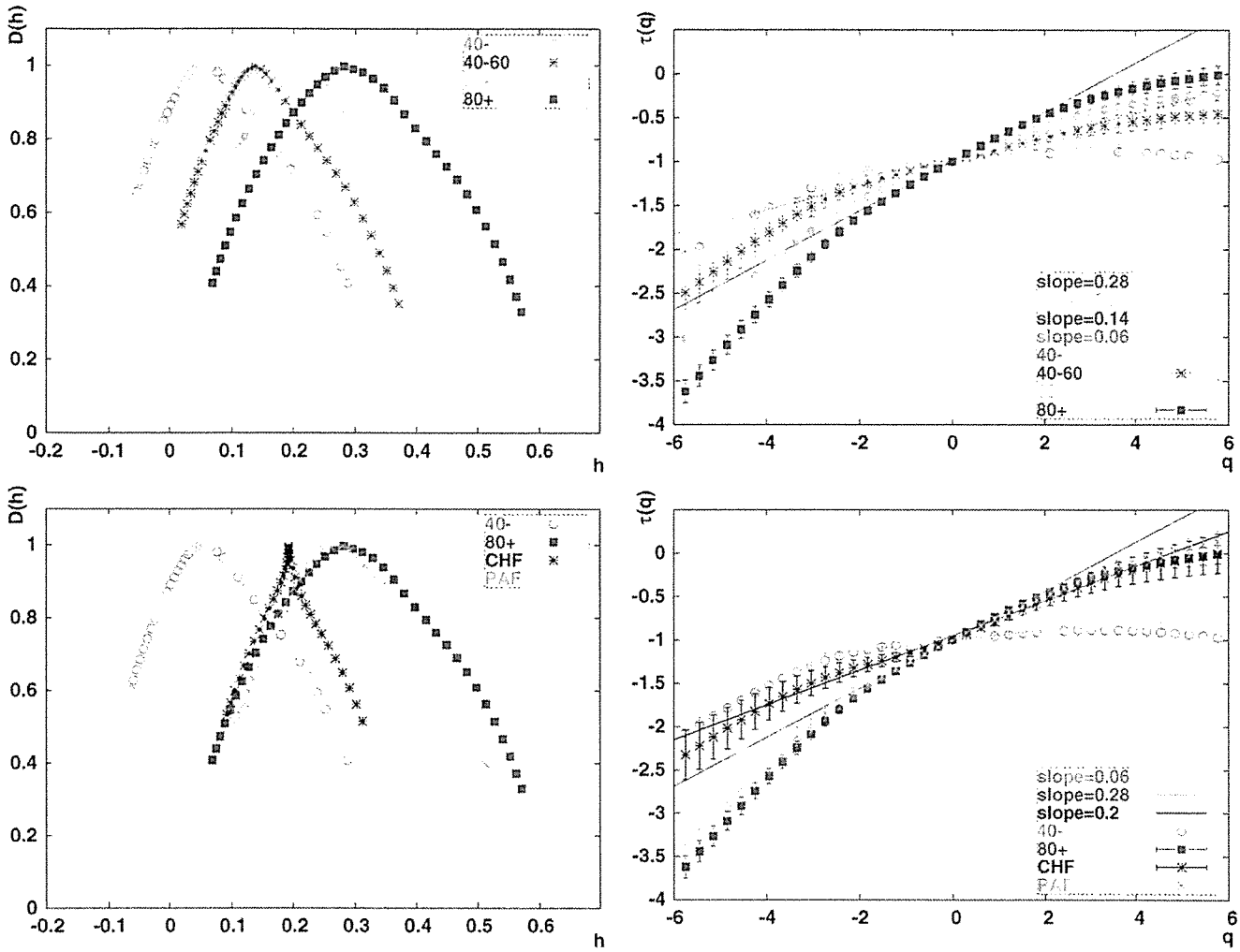

Fig. 3. Singularity spectra $D(h)$, together with the $\tau(q)$ spectra of moments of the partition function $Z_q(s)$, for four age groups of healthy subjects and for PAF patients. For reference, CHF and PAF spectra are also outlined [11]. Note the preserved width of $D(h)$, even for subjects in the oldest age group.

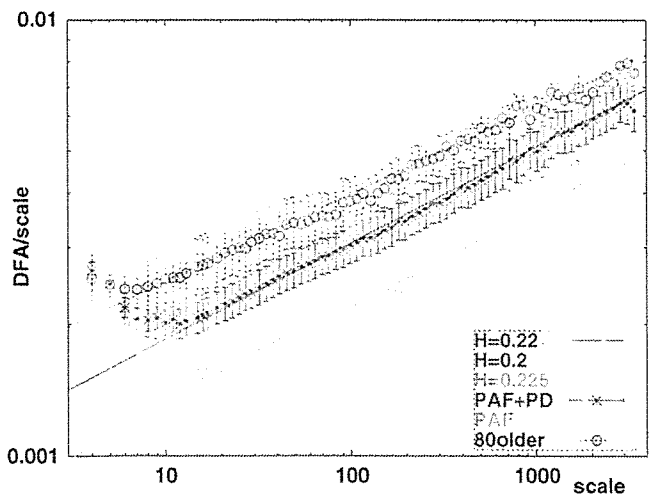

Fig. 4. Scale dependency of the mean detrended fluctuation $\bar{D}_{\mathrm{DFA}}(s)$ for the 80+ age group of healthy subjects and for both the PAF patients group and the "simulated autonomic aging" group (PAF + PD). Detrended fluctuations have been calculated with first-order DFA, i.e., linear trend removal [32]. The vertical bars represent the standard deviations of the group means.

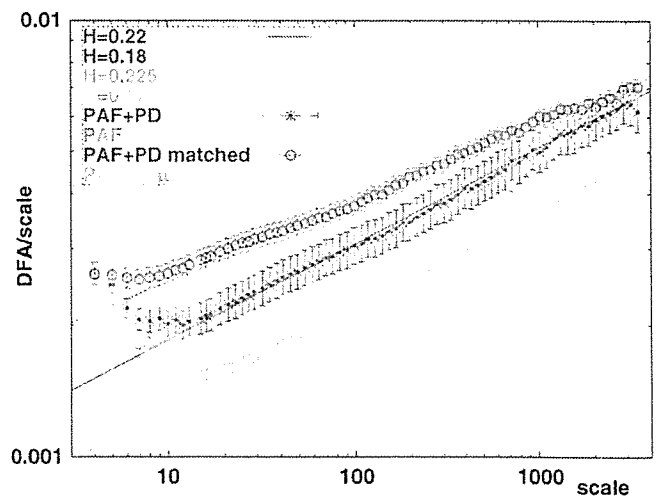

Fig. 5. Scale dependency of the mean detrended fluctuation $\bar{D}_{\mathrm{DFA}}(s)$ for both the PAF patients group and the "simulated autonomic aging" group (PAF+PD), compared with healthy subjects matched by age and gender with the patients in the two groups. Detrended fluctuations have been calculated with first-order DFA, i.e., linear trend removal [32]. The vertical bars represent the standard deviations of the group means.

of decreased SNS function as a manifestation of autonomic aging. It may be important to verify whether PD patients alone display "autonomic aging" tendencies. We consider this a likely possibility, however, it requires further research due to

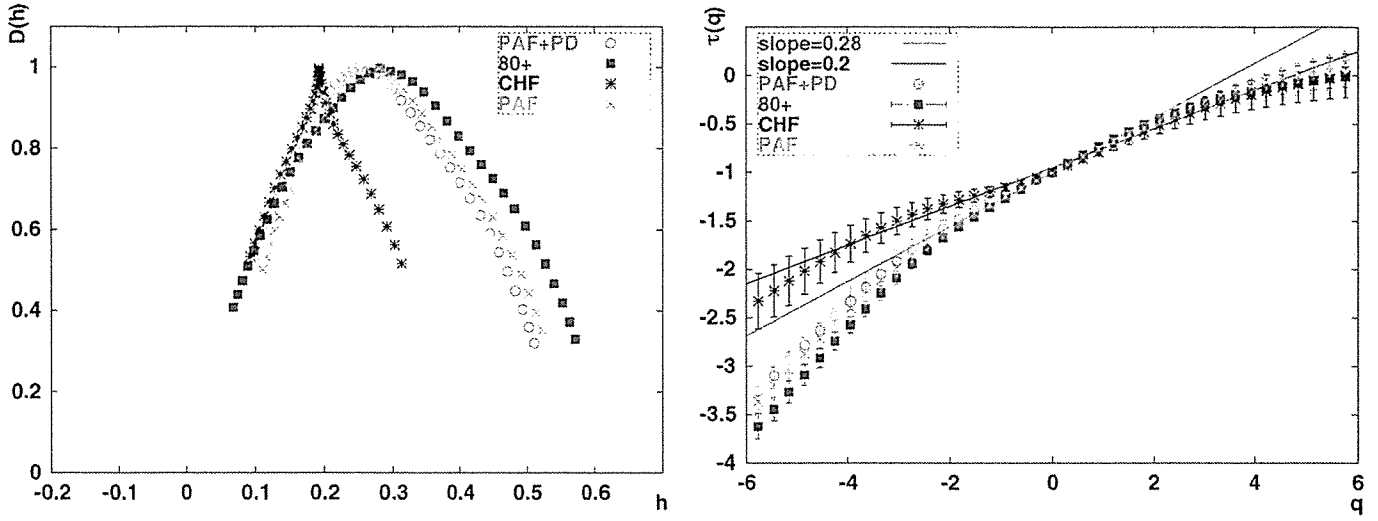

Fig. 6. Singularity spectra $D(h)$, together with the $\tau(q)$ spectra of moments of the partition function $Z_q(s)$, for the 80+ healthy subjects and for the PAF and the "simulated autonomic aging" group (PAF + PD) of patients. For reference, the CHF spectrum is also outlined [11].

the limited number of patients in the present study. If verified, this might provide an additional diagnostic window for this prevalent disorder.

VI. Conclusion

The systematic increase in long-range correlation and preserved multifractality of heart rate dynamics with aging, as well as in large-scale brain stem neurodegenerative disorders with the sympathetic dysfunction, suggest that aging is associated with a lack of SNS function, rather than the sympathetic overexcitation seen in, e.g., CHF, to cope dynamically with various environmental stimuli.

Acknowledgment

The authors wish to thank S. Sakata, K. Kiyono, N. Aoyagi, and K. Saito for their help and discussions.

References

[1] C. K. Peng, J. Mietus, J. M. Hausdorff, S. Havlin, H. E. Stanley, and A. L. Goldberger, "Long-range anticorrelations and non-Gaussian behavior of the heartbeat," *Phys. Rev. Lett.*, vol. 70, pp. 1343–1346, 1993.

[2] Y. Yamamoto and R. L. Hughson, "On the fractal nature of heart rate variability in humans: effects of data length and β-adrenergic blockade," *Am. J. Physiol.*, vol. 266, pp. R40–R49, 1994.

[3] P. C. Ivanov, L. A. N. Amaral, A. L. Goldberger, S. Havlin, M. G. Rosenblum, Z. R. Struzik, and H. E. Stanley, "Multifractality in human heart rate dynamics," *Nature*, vol. 399, pp. 461–465, 1999.

[4] L. A. N. Amaral, P. C. Ivanov, N. Aoyagi, I. Hidaka, S. Tomono, A. L. Goldberger, H. E. Stanley, and Y. Yamamoto, "Behavioral-independent features of complex heartbeat dynamics," *Phys. Rev. Lett.*, vol. 86, pp. 6026–6029, 2001.

[5] U. Frisch, *Turbulence*, 1st ed. Cambridge, U.K.: Cambridge Univ. Press, 1995.

[6] S. Ghashghaie, W. Breymann, J. Peinke, P. Talkner, and Y. Dodge, "Turbulent cascades in foreign exchange markets," *Nature*, vol. 381, pp. 767–770, 1996.

[7] P. Bak, C. Tang, and K. Wiesenfeld, "Self-organized criticality: an explanation of $1/f$ noise," *Phys. Rev. Lett.*, vol. 59, pp. 381–384, 1987.

[8] H. E. Stanley, "Scaling, universality, and renormalization: three pillars of modern critical phenomena," *Rev. Mod. Phys.*, vol. 71, pp. S358–S366, 1999.

[9] J. P. Sethna, K. A. Dahmen, and C. R. Myers, "Crackling noise," *Nature*, vol. 410, pp. 242–250, 2001.

[10] Y. Yamamoto, Y. Nakamura, H. Sato, M. Yamamoto, K. Kato, and R. L. Hughson, "On the fractal nature of heart rate variability in humans: effects of vagal blockade," *Am. J. Physiol.*, vol. 269, pp. R830–R837, 1995.

[11] Z. R. Struzik, J. Hayano, S. Sakata, S. Kwak, and Y. Yamamoto, "$1/f$ scaling in heart rate requires antagonistic autonomic control," *Phys. Rev. E*, vol. 70, 2004.

[12] L. A. Lipsitz and A. L. Goldberger, "Loss of 'complexity' and aging. Potential applications of fractal and chaos theory to senescence," *JAMA*, vol. 267, pp. 1806–1809, 1992.

[13] A. D. Jose and D. Collison, "The normal range and determinants of the intrinsic heart rate in man," *Cardiovasc. Res.*, vol. 4, pp. 160–167, 1970.

[14] T. Opthof, "The normal range and determinants of the intrinsic heart rate in man," *Cardiovasc. Res.*, vol. 45, pp. 177–184, 2000.

[15] M. Bursztyn, M. Bresnahan, I. Gavras, and H. Gavras, "Effect of aging on vasopressin, catecholamines, and α_2-adrenergic receptors," *J. Am. Geriatrics Soc.*, vol. 38, pp. 628–632, 1990.

[16] D. C. Shannon, D. W. Carley, and H. Benson, "Aging of modulation of heart rate," *Am. J. Physiol.*, vol. 253, pp. H874–H877, 1987.

[17] J. B. Schwartz, W. J. Gibb, and T. Tran, "Aging effects on heart rate variability," *J. Gerontol.*, vol. 46, pp. M99–M106, 1991.

[18] K. Jensen-Urstad, N. Storck, F. Bouvier, M. Ericson, L. E. Lindblad, and M. Jensen-Urstad, "Heart rate variability in healthy subjects is related to age and gender," *Acta Physiol. Scand.*, vol. 160, pp. 235–241, 1997.

[19] C. Fukusaki, K. Kawakubo, and Y. Yamamoto, "Assessment of the primary effect of aging on heart rate variability in humans," *Clin. Auton. Res.*, vol. 10, pp. 123–130, 2000.

[20] A. Malliani, M. Pagani, F. Lombardi, and S. Cerutti, "Cardiovascular neural regulation explored in the frequency domain," *Circulation*, vol. 84, pp. 482–492, 1991.

[21] J. P. Saul, "Beat-to-beat variations of heart rate reflect modulation of cardiac autonomic outflow," *News Physiol. Sci.*, vol. 5, pp. 32–37, 1990.

[22] D. T. Kaplan, M. I. Furman, S. M. Pincus, S. M. Ryan, L. A. Lipsitz, and A. L. Goldberger, "Aging and the complexity of cardiovascular dynamics," *Biophys. J.*, vol. 59, pp. 945–949, 1991.

[23] N. Iyengar, C. K. Peng, R. Morin, A. L. Goldberger, and L. A. Lipsitz, "Age-related alterations in fractal scaling of cardiac interbeat interval dynamics," *Am. J. Physiol.*, vol. 271, pp. R1078–R1084, 1996.

[24] S. M. Pikkujämsä, T. H. Mäkikallio, L. B. Sourander, I. J. Räihä, P. Puukka, J. Skyttä, C. K. Peng, A. L. Goldberger, and H. V. Huikuri, "Cardiac interbeat interval dynamics from childhood to senescence. Comparison of conventional and new measures based on fractals and chaos theory," *Circulation*, vol. 100, pp. 393–399, 1999.

[25] M. G. Kienzle, D. W. Ferguson, C. L. Birkett, G. A. Myers, W. J. Berg, and D. J. Mariano, "Clinical, hemodynamic and sympathetic neural correlates of heart rate variability in congestive heart failure," *Am. J. Cardiol.*, vol. 69, pp. 761–767, 1992.

[26] M. Elam, Y. B. Sverrisdottir, D. M. B. Rundqvist, B. G. Wallin, and V. G. Macefield, "Pathological sympathoexcitation: how is it achieved?," *Acta Physiol. Scand.*, vol. 177, pp. 405–411, 2003.

[27] J. P. Saul, Y. Arai, R. D. Berger, L. S. Lilly, W. S. Colucci, and R. J. Cohen, "Assessment of autonomic regulation in chronic congestive heart failure by heart rate spectral analysis," *Am. J. Cardiol.*, vol. 61, pp. 1292–1299, 1988.

[28] D. R. Oppenheimer, "Lateral horn cells in progressive autonomic failure," *J. Neurol. Sci.*, vol. 46, pp. 393–404, 1980.
[29] M. R. Matthew, "Autonomic ganglia and preganglionic neurons in autonomic failure," in *Autonomic Failure*, 4th ed, C. J. Mathias and R. Bannister, Eds. Oxford, U.K.: Oxford Univ. Press, 1999, pp. 329–339.
[30] S. Sakata, J. Hayano, S. Mukai, A. Okada, and T. Fujinami, "Aging and spectral characteristics of the nonharmonic component of 24-h heart rate variability," *Am. J. Physiol.*, vol. 276, pp. R1724–R1731, 1999.
[31] N. Aoyagi, K. Ohashi, S. Tomono, and Y. Yamamoto, "Temporal contribution of body movement to very long-term heart rate variability in humans," *Am. J. Physiol. Heart Circ. Physiol.*, vol. 278, pp. H1035–H1041, 2000.
[32] C. K. Peng, S. Havlin, H. E. Stanley, and A. L. Goldberger, "Quantification of scaling exponents and crossover phenomena in nonstationary heartbeat time series," *Chaos*, vol. 5, pp. 82–87, 1995.
[33] A. L. Goldberger, L. A. N. Amaral, L. Glass, S. Havlin, J. M. Hausdorff, P. C. Ivanov, R. G. Mark, J. E. Mietus, G. B. Moody, C. K. Peng, and H. E. Stanley, "PhysioBank, PhysioToolkit, and PhysioNet: components of a new research resource for complex physiologic signals," *Circulation*, vol. 101, pp. e215–e220, 2000.
[34] J. F. Muzy, E. Bacry, and A. Arneodo, "The multifractal formalism revisited with wavelets," *Int. J. Bifurc. Chaos*, vol. 4, pp. 245–302, 1994.
[35] T. Vicsek, *Fractal Growth Phenomena*, 2nd ed, Singapore: World Scientific, 1993.
[36] K. P. Davy, D. R. Seals, and H. Tanaka, "Augmented cardiopulmonary and integrative sympathetic baroreflexes but attenuated peripheral vasoconstriction with age," *Hypertension*, vol. 32, pp. 298–304, 1998.
[37] A. M. Palmer and S. T. DeKosky, "Monoamine neurons in aging and Alzheimer's disease," *J. Neural Transmission*, vol. 91, pp. 135–159, 1993.
[38] D. A. Bennet, L. A. Beckett, A. M. Murray, K. M. Shannon, C. G. Goetz, D. M. Pilgrim, and D. A. Evans, "Prevalence of parkinsonian signs and associated mortality in community population of older people," *N. Engl. J. Med.*, vol. 334, pp. 71–76, 1996.
[39] C. Zarow, S. A. Lyness, J. A. Mortimer, and H. C. Chui, "Neuronal loss is greater in the locus coeruleus than nucleus basalis and substantia nigra in Alzheimer and Parkinson diseases," *Arch. Neurol.*, vol. 60, pp. 337–341, 2003.
[40] S. Orimo, E. Ozawa, S. Nakade, T. Sugimoto, and H. Mizusawa, "^{123}I-metaiodobenzylguanidine myocardial scintigraphy in Parkinson's disease," *J. Neurol. Neurosurg. Psych.*, vol. 67, pp. 189–194, 1999.

Junichiro Hayano graduated from Nagoya City University Medical School, Nagoya, Japan, and received the M.D. degree in 1980. From 1981 to 1983, he received residency training in psychosomatic medicine at Kyushu University School of Medicine, Fukuoka, Japan. He received the Ph.D. degree (Dr. of Medical Science) in 1988 from Nagoya City University Graduate School of Medical Sciences on the basis of a thesis on the "Assessment of autonomic nervous functions by heart rate variability."

From 1990 to 1991, he worked as a visiting associate at the Behavioral Medicine Research Center, Duke University Medical Center, Durham, NC, mainly on signal processing for ambulatory electrocardiography. In 1984, he was granted a faculty position at Nagoya City University Medical School and has been a Professor of Medicine at Nagoya City University Graduate School of Medical Sciences since 2003. His current interests are applications of dynamic electrocardiography and ambulatory monitoring to clinical cardiology and cardiovascular physiology.

Rika Soma received the Ph.D. degree from the University of Tokyo, Tokyo, Japan, in 1996.

From 1997 to 1999, she worked as a research associate at the University of Tsukuba, Tsukuba, Japan. She is currently a postdoctoral researcher at the University of Tokyo. Her fields of interest include the modification of the cardiovascular control system by vestibular stimulation in humans.

Shin Kwak was born in Tokyo, Japan, in 1951. He received the M.D degree from the University of Tokyo, Tokyo, in 1977. He received the Ph.D. degree in medical science from the University of Tokyo in 1984.

In 1984, he got a faculty position at the Department of Neurology, University of Tokyo Hospital. From 1986 to 1987, he worked as a guest scientist at Friedrich-Mischer Institut in Basel. He has been a Full Associate Professor at the Department of Neurology, Graduate School of Medicine, the University of Tokyo since 1997, where he is seeing patients, teaching undergraduate and graduate students, and researching on neurodegenerative diseases. His current interests lie in elucidating the pathogenic mechanism and developing specific therapeutic strategy for amyotrophic lateral sclerosis where he found that RNA editing of AMPA receptor is deficient.

Dr. Kwak was board certified in neurology in 1981.

Zbigniew R. Struzik received the M.S. degree in technical physics from the Technical University of Warsaw, Warsaw, Poland, in 1986, and the Doctor of Science degree from the University of Amsterdam, Amsterdam, The Netherlands, in 1996.

Between 1997 and 2003, he worked at the Center for Mathematics and Computer Science (CWI), Amsterdam. His scientific work contributed to the amalgamation of (multi-)fractal analysis, wavelet analysis and time series data mining. He is currently working as an Associate Research Professor at the University of Tokyo, Japan. His research interests include (multi-)fractals, complex systems, time series processing and mining, and, in particular, applications of the wavelet transformation. He is on the editorial board of the *Fractals Journal*, on the reviewers' board of the *Data and Knowledge Engineering Journal* and is a Database Expert Systems Applications (DEXA) program committee member.

Yoshiharu Yamamoto was born in Tokyo, Japan, in 1960. He received the Ph.D. degree in education from the University of Tokyo, Tokyo, Japan, in 1990.

From 1989 to 1993, he was working as a Postdoctoral Researcher at the Department of Kinesiology, University of Waterloo, Waterloo, ON, Canada, mainly on biosignal processing for human cardiovascular physiology. In 1993, he got a faculty position at the Graduate School of Education, the University of Tokyo, and has been a Full Professor at the Educational Physiology Laboratory, Graduate School of Education, the University of Tokyo since 2000, where he is teaching and researching physiological bases of health sciences and education. His current interests lie in biomedical signal processing, nonlinear and statistical bio-dynamics, and regulatory physiology. See http://www.p.u-tokyo.ac.jp/~yamamoto/yycve/yycve.html, for details.

Movement Disorders
Vol. 00, No. 0, 2007, pp. 000–000
© 2007 Movement Disorder Society

Power-Law Temporal Autocorrelation of Activity Reflects Severity of Parkinsonism

AQ: 1

Weidong Pan,[1] Kyoko Ohashi,[2,3] Yoshiharu Yamamoto,[2] and Shin Kwak[1]*

[1]*Department of Neurology, Graduate School of Medicine, The University of Tokyo, Tokyo, Japan*
[2]*Educational Physiology Laboratory, Graduate School of Education, The University of Tokyo, Tokyo, Japan*
[3]*Developmental Biopsychiatry Research Program, McLean Hospital/Harvard Medical School, Belmont, Massachusetts, USA*

Abstract: We aimed to obtain a reliable, objective scale representing disease severity for appropriate management of patients with Parkinson's disease (PD). Nineteen patients with PD at the Department of Neurology, Tokyo University Hospital, were classified into mild (n = 10) or severe groups (n = 9) depending on their Hoehn-Yahr scores, and wore accelerometers on their wrists for more than 6 consecutive days. During this time we monitored their subjective assessments of symptom severity and analyzed the power-law exponents (α) for local maxima and minima of fluctuations in the activity time series. Statistical comparisons were made between the severe and mild groups and of individual patients on "good condition" and "bad condition" days, as well as between days before and after antiparkinsonism medication. In all patients, the α for local maxima was always lower when parkinsonism was mild than when severe. Presence of tremor did not influence the α for local maxima. As the lower α value for local maxima of fluctuations in activity records reflects more frequent switching behavior from low to high physical activities or the severity of akinesia, actigraph monitoring of parkinsonism, and analysis of its power-law correlation may provide useful objective information for controlling parkinsonism in outpatient clinics and for evaluating new antiparkinsonism drugs. © 2007 Movement Disorder Society

Key words: Parkinson's disease; actigraph; akinesia; fractal analysis; power-law temporal autocorrelation.

A reliable objective scale representing disease severity is necessary for appropriate management of Parkinson's disease (PD) patients. Although the Unified Parkinson's Rating Scale (UPDRS)[1] is a standard method for evaluating parkinsonism severity, UPDRS scores may not adequately reflect the disease severity. Wearable accelerometers (such as an actigram AMI, Ambulatory Monitors USA) enable long-term recording of patient's movement during activities of daily living, and hence might be the best choice for a device for quantitative assessment of the symptoms due to various diseases.[2-8] Recently, studies have been successful in developing reliable analytical methods that quantitatively represent the disease progression in patients with tremor.[9-11] Here, an analytical method sufficiently sensitive and reliable to represent the severity of non-tremor activity is presented.

Recently, fractal analysis was shown to be a robust tool to disclose hidden autocorrelation patterns in biological data, such as heartbeat and limb movement.[12-17] Power-law autocorrelation exponents for local maxima and minima of fluctuations of locomotor activity would be the most useful for our purpose, as they represent the level of persistency of movement patterns. In this study, we analyzed patients' physical activity records collected by an actigraph device using power-law exponents probing temporal autocorrelation of the activity counts. We found that the power-law exponent for local maxima most sensitively and reliably reflects disability without being influenced by the presence of tremor or the patterns of daily living.

PATIENTS AND METHODS

Nineteen patients with PD (13 male and 6 female; mean age ± SEM, 63.7 ± 9.8 years) at the Department of Neurology of the Tokyo University Hospital partici-

*Correspondence to: Dr. Shin Kwak, Department of Neurology, Graduate School of Medicine, The University of Tokyo, 7-3-1 Hongo, Bunkyo-ku, Tokyo 113-8655, Japan. E-mail: kwak-tky@umin.ac.jp
Received 27 December 2006; Revised 16 March 2007; Accepted 19 March 2007
Published online 00 Month 2007 in Wiley InterScience (www.interscience.wiley.com). DOI: 10.1002/mds.21527

48

tapraid5/za2-mds/za2-mds/za200707/za22061d07o | sangreyj | S=10 | 4/10/07 | 21:31 | Art: 21527 | Input-yyy(v)

TABLE 1. *The profile of subjects*

Patients	Age (year)	Sex	Hoehn and Yahr score		Duration of illness (year)	Tremor
			On	Off		
Pt. 1	54	M	2.0	3.0	5	+
Pt. 2	72	F	2.5	3.0	4	
Pt. 3	41	F	2.0	2.5	7	
Pt. 4	70	M	2.5	3.0	9	+
Pt. 5	57	M	2.0	2.5	10	
Pt. 6	60	F	1.5	2.0	5	
Pt. 7	65	M	1.5	2.0	5	
Pt. 17	57	M	1.0	1.5	1.5	+
Pt. 18	42	M	1.5	2.0	8	−
Pt. 19	71	M	2.0	2.5	8	
Mean ± SEM	*58.9 ± 3.52*		*1.85 ± 0.15*	*2.4 ± 0.16*	*6.25 ± 0.82*	
Pt. 8	60	F	3.5	4.5	6	−
Pt. 9	64	F	3.0	4.0	8	+
Pt. 10	60	M	3.0	4.0	10	−
Pt. 11	64	M	3.0	4.0	5	
Pt. 12	70	M	4.0	4.5	10	+
Pt. 13	79	F	3.5	4.0	12	−
Pt. 14	60	M	3.0	3.5	20	−
Pt. 15	57	M	3.5	4.0	8	+
Pt. 16	73	M	4.0	4.5	7	
Mean ± SEM	*65.22 ± 2.43*		*3.39 ± 0.14*	*4.11 ± 0.11*	*9.56 ± 1.49*	

Controls	Age (year)	Sex	Property	Profession
Con. 1	36	M	Healthy	Student
Con. 2	51	M	Healthy	Professor
Con. 3	28	F	Healthy	Technician
Con. 4	50	F	Healthy	Manager
Con. 5	32	M	Healthy	Student
Con. 6	30	F	Healthy	Student
Mean ± SEM	*37.83 ± 4.15*			

T1

pated in this study (Table 1). Depending on their Hoehn and Yahr scores, the patients were classified into mild (>3, mean ± SEM, 2.13 ± 0.13) or severe groups (>3, 3.75 ± 0.12). Three patients in the mild group and 3 in the severe group had resting tremor but only on their dominant sides. Patients had no overt dementia or depression. Six healthy control patients (3 female and 3 male; 37.8 ± 4.2 years) were recruited from volunteers at The University of Tokyo. The study was approved by The Ethics Committee of the Graduate School of Medicine, The University of Tokyo, and performed under the principles outlined in the Declaration of Helsinki.

A small, custom wristwatch-sized activity monitor, ECOLOG (ECOlogical neurobehavior LOGger), equipped with a computer (Ruputer Pro, Seiko Instruments, Chiba, Japan) was used in this study to register and quantify human physical activity. In its Zero-crossing mode (ZCM), the zero-crossing counts were integrated over 1-minute intervals and the data was stored in internal memory. The activity monitoring device is analogous in performance to the commercial Actigraph Mini-Motionlogger (Ambulatory Monitors, Ardsley, NY) which has frequently been used for studies of physical activity[2,18,19]; the correlation coefficient between activity counts measured simultaneously by both devices for 24 hours was 0.91 ± 0.02 and for awake-time alone 0.82 ± 0.03 (mean ± SD, n = 6) in healthy adults (Y. Yamamoto, unpublished observation). In this study, we recorded activity counts/min in the ZCM with a setting comparable to mode 13 of the Mini-Motionlogger (filter range of acceleration signals: 2–3 Hz, sensitive threshold: high, gain: low). After recording, data were transmitted to an external computer by software installed on the device.

Participants wore the ECOLOG on the wrist of their nondominant side, or on some occasions on both sides, for more than 6 consecutive days. Patients were asked to keep a diary in which they recorded their disability grade every 30 minutes. The diary scores were defined as follows: 0 (almost no activity), 1 (very difficult to initiate movement), 2 (difficulty in initiating movement), 3 (some difficulty in activities in daily living), and 4 (almost normal). They were also asked to write down the time they took pills and periods when they removed the ECOLOG. Because most of the patients could manage their daily living by themselves and reported feeling good when the proportion of diary scores at ≥3 exceeded 60% of the awake-time, we arbitrary classified the days

into two categories based on this proportion; when more than 60% of the awake-time was scored as ≥3, the day was defined as a "good condition" (GC) day, and when less than 60% of the awake-time was ≥3, the day was defined as a "bad condition" (BC) day. Six of the PD patients, whose diagnoses included MRI findings, and who had not received any antiparkinsonism drugs wore the ECOLOG for more than 6 consecutive days both before the initiation of medication and after the stabilization of medication effects (Pt. 1, 2, 6, 7, 17, 18). The "after" study was conducted when the dose of the medication (2–3 mg of cabergoline or 0.45–0.75 μg of pergolide) was stable for more than 3 weeks in each patient.

We separated the data acquired during awake-time and sleep-time with Action-W, Version 2 (Ambulatory Monitors, Ardsley, NY) and the data during awake-time were used for analyses. To examine temporal autocorrelation of the physical activity time series (i.e., dynamic aspects of physical activity) we used an extended, random-walk analysis, the detrended fluctuation analysis (DFA),[13] with a recent modification[12] for various "real-world" signals including activity time series. The original DFA evaluates relationships between time scales and magnitudes of fluctuation (standard deviations) within each time scale; more correlated signals represent a greater growth of the fluctuation magnitude with increasing time scale or length of data window. It also eliminates nonstationarity in the input data (i.e., changes in the baseline and trends within the data windows at different scales) that could affect calculation of the magnitudes of fluctuation, thus making this approach suitable for the analysis of the long-term data collected in the present study. The power-law (scaling) exponent (α), obtained as the slope of a straight line fit in the double-logarithmic plot of time scales versus magnitudes of fluctuation, was used to characterize the level of such correlation. This index reflects the probability of a simultaneous increase or decrease in the variability at two distant points in time in the time series, applied to all distances up to long-range time scales, thereby probing the nature of "switching" patterns between high and low values in a statistical sense. Larger power-law exponents indicate positive temporal autocorrelation or persistency in the increase or decrease, and lower values correspond to negative autocorrelation or antipersistency.

Recently, Ohashi et al. reported that physical activity data have different power-law exponents in periods with higher and lower activity levels, corresponding to qualitatively different physiological states, (i.e., active and rest, respectively).[12] The actual procedures we used are as follows: (see Ohashi et al. for details).[12] First, a

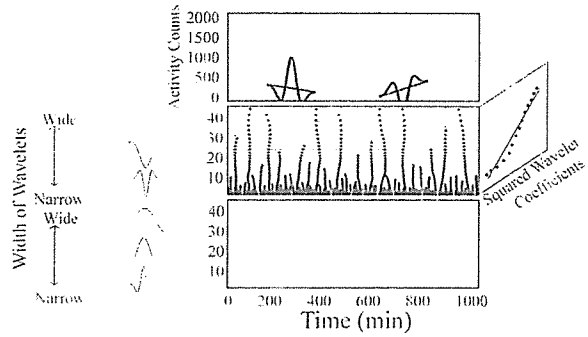

FIG. 1. Conceptual explanation of the method to obtain power-law exponents for local maxima and minima. (top) Various widths of hat-shaped wavelets are slid along the data to detect local minima (middle) and local maxima (bottom) of the wavelet coefficients. Note that the local minima and maxima appear at the transient decreases and increases of the activity, respectively. The power-law exponents are calculated from the slope of the log-log plot of squared wavelet coefficients versus the scale for local minima and maxima. In the actual analysis, we used an integrated, rather than raw, time series and $\psi(t)$, i.e., the derivative of the "hat-shaped" wavelet. This yields the same power-law exponents as those obtained by the DFA method for the same local maxima and minima as obtained in this figure (see Methods for details).

daytime physical activity time series was integrated, as in DFA, and wavelets with different time scales (S) were slid along the time series and correlated with the data to obtain the wavelet coefficients ($W(S)$) at each point. We used the third derivative of the Gaussian function as the so-called "mother wavelet":

$$\psi(t) = t(3 - t^2)e^{-0.5t^2},$$

where t is time. This is equivalent to using the Gaussian second derivative (so-called "Mexican hat") wavelet to examine the raw signals (Fig. 1), though the integration approach automatically removes the local mean and the local linear trend, as in DFA. By changing the scale of the wavelet, this "hat-shaped" template dilates or contracts in time, probing transient increases or decreases in activity records in different time scales. The transient increases (low-high-low activity patterns) yield local maxima of the wavelet coefficients at their time points, while the decreases (high-low-high activity patterns) yield local minima of the wavelet coefficients (Fig. 1). Next, the squared wavelet coefficients at the local maxima or minima were averaged for all the available days. As the coefficient gives the magnitude of local fluctuations matching the shape of $\psi(t)$ with different time scales, the squared $W(S)$ was used, again as in DFA. Finally, the power-law exponent (α) was obtained separately for local maxima and minima as the slope of a straight line fit in the double-logarithmic plot of S versus

F1

tapraid5/za2-mds/za2-mds/za200707/za22061d07o | sangreyj | S=10 | 4/10/07 | 21:31 | Art: 21527 | Input-yyy(v)

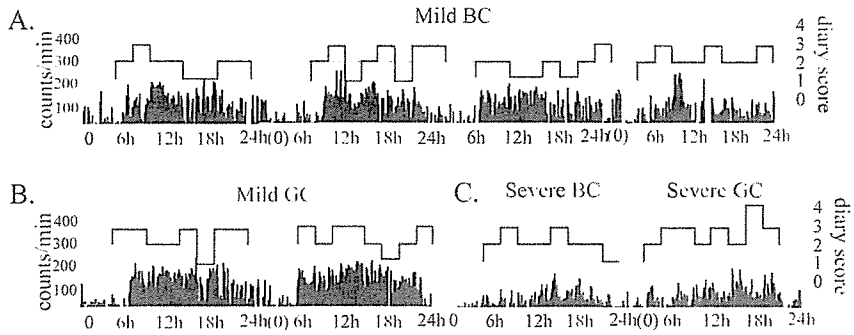

FIG. 2. Examples of daily activity profiles and the corresponding subjective, diary-based scoring on days in different conditions in patients with different disease severities. BC, bad condition day; GC, good condition day.

$W(S)^2$. In this study, the range of S corresponding to 8 to 35 minutes, where acceptable linear relationships between log S and log $W(S)^2$ were observed for all the records, was used. This range is also approximately the same as that used in Ohashi et al.[12] Note that this method yields the same α-values as does DFA,[20] but separately for periods with higher and lower activity levels. The power-law exponent α's of local maxima and minima were used to assess the quantitative disabilities during awake-time and the differences in disabilities between GC days and BC days, between before and after antiparkinsonism medication in individuals, between the severe and mild groups, and between groups with and without tremor. Records during 6 consecutive days were used in the analysis.

Wilcoxon signed rank tests were performed to compare α-values for local maxima or minima in the various group comparisons. P values < 0.05 were considered statistically significant.

RESULTS

The daily profile of physical activity exhibited robust activity-rest cycles but no apparent correspondence between daily activity profiles and diary scores (the mean activity counts vs. diary score: r = −0.063) (Fig. 2). F2

Average wavelet coefficients for local maxima and minima of the severe and mild groups provided straight lines in the range of 8 to 35 minutes (Fig. 3A), indicative F3 of very robust α-values. When the mean α-values for local maxima and minima were compared, we found a significantly lower α-value for local maxima in the mild group than in the severe group (Fig. 3B). All the patients in both the severe and mild groups showed significantly lower α-values for local maxima on GC days than on BC days, whereas there was no significant difference in the mean α-values for local minima (Fig. 3C). When the effects of medication were examined, we found that all the patients showed lower α-values for local maxima, but

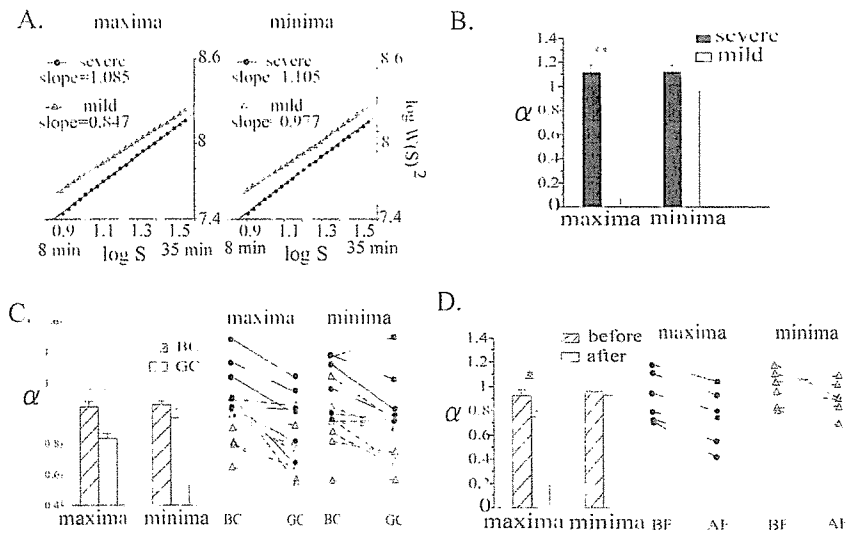

FIG. 3. Local maxima and minima of fluctuation of physical activity. (A) Average wavelet coefficients, as a function of the wavelet scale, for local maxima and minima. The slopes are power-law exponents, α. (B) Comparisons of the mean α for the severe and the mild groups, (C) for BC and GC days and for individual patients, and (D) for days before and after antiparkinsonism medication and for each patient. *$P < 0.05$, **$P < 0.01$, and ***$P < 0.001$.

tapraid5/za2-mds/za2-mds/za200707/za22061d07o | sangreyj | S=10 | 4/10/07 | 21:31 | Art: 21527 | Input-yyy(v)

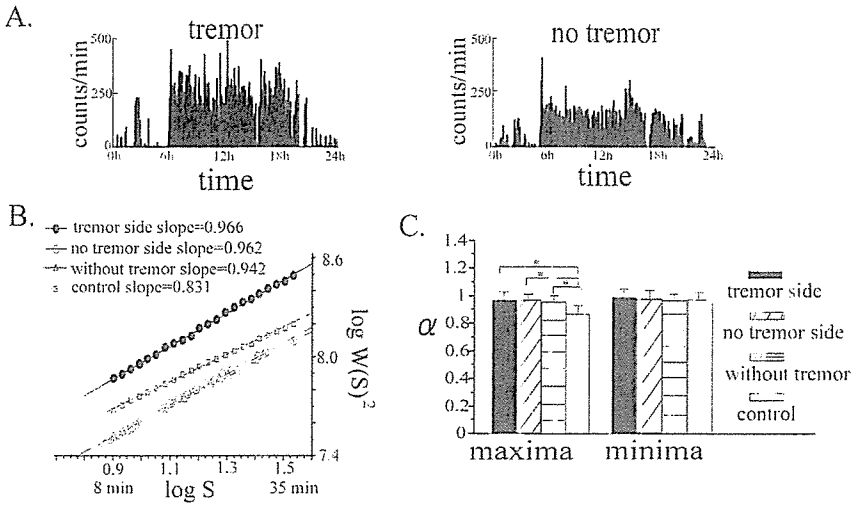

FIG. 4. Effects of tremor. (A) Daily profiles of physical activity for the arm affected with tremor and that without tremor of a patient with unilaterally predominant parkinsonism with continuous tremor on one side. (B) Average wavelet coefficients for local maxima among arms with tremor (tremor) and without tremor (no tremor). Arms of patients with tremor (n = 6), arms of patients without tremor (without tremor: n = 13), and control subjects (control: n 6). (C) The power-law exponents for local maxima and minima. *$P < 0.05$.

not for local minima, on days after they received anti-parkinsonism medication than on those before (Fig. 3D).

We compared the activity records from the arms with tremor and without tremor from 6 patients with tremor, and arms of patients not affected with tremor (n = 13). The activity counts in the arms with tremor were significantly higher than those in the arms without tremor (Fig. 4A). Power-law scaling of the records from arms with tremor showed a linear correlation between log S and log $W(S)^2$ in the range of 8 to 35 minutes (Fig. 4B) and α-values for local maxima but not for minima were significantly higher in patient arms than in control arms irrespective of tremor (Fig. 4C)

DISCUSSION

We demonstrated that analysis of records of a custom actigraph by the power-law temporal correlation is a powerful tool for the quantitative evaluation of physical activity in patients with parkinsonism. The diary-based subjective scoring of good or BCs was apparently not correlated with the objective daily profiles of physical activity recorded by the accelerometer, indicating that the activity counts themselves do not represent the patient's condition.

Larger power-law exponents (α) indicate positive temporal autocorrelation, or persistency, in the increase or decrease in the variability of activity at two distant points in time in the time series, and lower values correspond to negative autocorrelation or anti-persistency.[12] In other words, a lower α for local maxima or minima of activity records reflects more frequent switching behavior from low to high or high to low physical activity, respectively, and the switching behavior from lower to higher activity levels is considered to be related to akinesia in patients with parkinsonism. We found lower α-values for local maxima during GC days than during BC days, in the mild group than in the severe group, and before medication than after medication. Thus, these results demonstrate that the power-law analyses accurately describe the well known phenomenon that under these conditions patients switch their physical activity from lower to higher levels more easily, in other words they exhibit milder akinesia, when the parkinsonism is mild than when it is severe. It is worthy to note that lower α-values for local maxima were obtained for all the patients after medication than before, and when in GC than in BC, thereby providing a temporal profile of parkinsonism in each individual patient.

We adopted Mode 13 of the ECOLOG to record the motion range during daily living. This is compatible with the same mode of the AMI Mini-Motionlogger and is said to filter out the majority of movements with frequencies outside the 2 to 3 Hz range. Although some resting tremor in the 4 to 8 Hz range, found in typical parkinsonism or in a part of the "true " movement accelerations resulting from muscle force[21] might have been filtered out of our recordings, we found higher activity counts during awake-time on the arms with tremor, which erroneously indicated milder parkinsonism compared with the arms without tremor when judged from the level of activity counts. In contrast, the α-values for local maxima did not differ between the arms with tremor and those without tremor, but were significantly lower in both of the patient groups than in the control arms, indicating that although the presence of tremor

greatly influenced the actigraphic counts, the presence of tremor did not yield false positive results in the power-law exponent for maxima.

In conclusion, we found that the power-law exponent for local maxima sensitively and reliably reflects disability without being influenced by the presence of tremor or the pattern of daily living. Our results thus suggest that analysis of power-law temporal autocorrelation of physical activity time series using the bidirectional extension[12] is applicable to patients with parkinsonism for the evaluation of akinesia irrespective of the presence of involuntary movements including tremor and may provide useful objective data necessary for the control of drug dosage in the outpatient clinic and also for the evaluation of new drugs for parkinsonism.

Acknowledgments: This study was financially supported by a grant from the Ministry of Health, Labor and Welfare of Japan and a contribution from Ms. Shigeko Moriyama. We thank Dr. Toru Nakamura at Osaka University for his help in validating the ECOLOG against the actigraph mini-motion logger.

REFERENCES

1. Martinez-Martin P, Gil-Nagel A, Gracia LM, et al. Unified Parkinson's Disease Rating Scale characteristics and structure. The Cooperative Multicentric Group. Mov Disord 1994;9:76-83.
2. Katayama S. Actigraph analysis of diurnal motor fluctuations during dopamine agonist therapy. Eur Neurol 2001;46 (Suppl 1):11-17.
3. Korte J, Hoehn T, Siegmund R. Actigraphic recordings of activity-rest rhythms of neonates born by different delivery modes. Chronobiol Int 2004;21:95-106.
4. van Someren EJ, Hagebeuk EE, Lijzenga C, et al. Circadian rest-activity rhythm disturbances in Alzheimer's disease. Biol Psychiatry 1996;40:259-270.
5. Okawa M, Mishima K, Hishikawa Y, Hozumi S. [Rest-activity and body-temperature rhythm disorders in elderly patients with dementia—senile dementia of Alzheimer's type and multi-infarct dementia]. Rinsho Shinkeigaku 1995;35:18-23.
6. Teicher MH. Actigraphy and motion analysis: new tools for psychiatry. Harv Rev Psychiatry 1995;3:18-35.
7. Mormont MC, Waterhouse J. Marked 24-h rest/activity rhythms are associated with better quality of life, better response, and longer survival in patients with metastatic colorectal cancer and good performance status. Clin Cancer Res 2000;6:3038-3045.
8. Tuisku K, Holi MM, Wahlbeck K, et al. Quantitative rest activity in ambulatory monitoring as a physiological marker of restless legs syndrome: a controlled study. Mov Disord 2003;18:442-448.
9. van Someren EJ, van Gool WA, Vonk BF, et al. Ambulatory monitoring of tremor and other movements before and after thalamotomy: a new quantitative technique. J Neurol Sci 1993; 117:16-23.
10. van Someren EJ, Vonk BF, Thijssen WA, et al. A new actigraph for long-term registration of the duration and intensity of tremor and movement. IEEE Trans Biomed Eng 1998;45:386-395.
11. Van Someren EJ, Pticek MD, Speelman JD, et al. New actigraph for long-term tremor recording. Mov Disord 2006;21:1136-1143.
12. Ohashi K, Nunes Amaral LA, Natelson BH, Yamamoto Y. Asymmetrical singularities in real-world signals. Phys Rev E Stat Nonlin Soft Matter Phys 2003;68:065204.
13. Peng CK, Havlin S, Stanley HE, Goldberger AL. Quantification of scaling exponents and crossover phenomena in nonstationary heartbeat time series. Chaos 1995;5:82-87.
14. Sekine M, Akay M, Tamura T, et al. Fractal dynamics of body motion in patients with Parkinson's disease. J Neural Eng 2004; 1:8-15.
15. Struzik ZR, Hayano J, Soma R, et al. Aging of complex heart rate dynamics. IEEE Trans Biomed Eng 2006;53:89-94.
16. Struzik ZR, Hayano J, Sakata S, et al. 1/f Scaling in heart rate requires antagonistic autonomic control. Phys Rev E Stat Nonlin Soft Matter Phys 2004;70:050901.
17. Ivanov PC, Amaral LA, Goldberger AL, et al. Multifractality in human heartbeat dynamics. Nature 1999;399:461-465.
18. Mormont MC, Waterhouse J. Contribution of the rest-activity circadian rhythm to quality of life in cancer patients. Chronobiol Int 2002;19:313-323.
19. Satlin A, Teicher MH, Lieberman HR, et al. Circadian locomotor activity rhythms in Alzheimer's disease. Neuropsychopharmacology 1991;5:115-126.
20. Yamamoto Y, Struzik ZR, Soma R, et al. Noisy vestibular stimulation improves autonomic and motor responsiveness in central neurodegenerative disorders. Ann Neurol 2005;58:175-181.
21. Van Someren EJ, Lazeron RH, Vonk BF, et al. Gravitational artefact in frequency spectra of movement acceleration: implications for actigraphy in young and elderly subjects. J Neurosci Methods 1996;65:55-62.

Acta Neuropathol (2006) 112:597–603
DOI 10.1007/s00401-006-0122-4

ORIGINAL ARTICLE

Transferrin localizes in Bunina bodies in amyotrophic lateral sclerosis

Yuji Mizuno · Masakuni Amari · Masamitsu Takatama · Hitoshi Aizawa · Ban Mihara · Koichi Okamoto

Received: 21 June 2006 / Revised: 13 July 2006 / Accepted: 13 July 2006 / Published online: 5 August 2006
Springer-Verlag 2006

Abstract Transferrin, an iron-binding protein, plays an important role in the transport and delivery of circulating ferric iron to the tissues. Amyotrophic lateral sclerosis (ALS) is characterized by the presence of Bunina bodies, skein-like inclusions, Lewy body-like inclusions/round inclusions, and basophilic inclusions in the remaining anterior horn cells in the spinal cord. We examined transverse paraffin sections of lumbar spinal cords from 12 ALS cases including two ALS with dementia and two ALS with basophilic inclusions, using antibodies to human transferrin. The results demonstrated that transferrin localized in Bunina bodies and some of the basophilic inclusions. In contrast, skein-like inclusions and Lewy body-like inclusions or round inclusions did not show obviously detectable transferrin immunoreactivities. Our findings suggest that although the mechanisms underlying transferrin accumulation in Bunina bodies and basophilic inclusions are unknown, transferrin could be involved in forming these inclusions. Furthermore, following cystatin C, transferrin is the second protein that localizes in the Bunina bodies.

Keywords Amyotrophic lateral sclerosis · Basophilic inclusions · Bunina bodies · Cystatin C · Transferrin

Y. Mizuno (✉) · K. Okamoto
Department of Neurology, Gunma University Graduate School of Medicine, 3-39-22 Showa-machi, Maebashi, Gunma 371-8511, Japan
e-mail: mizunoy@med.gunma-u.ac.jp

M. Amari · M. Takatama
Department of Internal Medicine, Geriatrics Research Institute and Hospital, 3-26-8 Otomo-machi, Maebashi, Gunma 371-0847, Japan

H. Aizawa
First Department of Internal Medicine, Asahikawa Medical College, Asahikawa 078-8510, Japan

B. Mihara
Institute of Brain and Blood Vessels, Mihara Memorial Hospital, 366 Ota-machi, Isesaki, Gunma 372-0006, Japan

Introduction

Amyotrophic lateral sclerosis (ALS) is neuropathologically characterized by loss of motor neurons and occurrence of Bunina bodies [21, 23], skein-like inclusions (SLI) [9], and Lewy body-like inclusions (LBLI) [6, 7, 14] in the remaining anterior horn cells of the spinal cord. Bunina bodies [21] ranging from 2 to 5 μm are present alone or in series in anterior horn cells in ALS, and LBLI [7] are more often seen in familial ALS than in sporadic ALS. With respect to the definition of LBLI, some authors have suggested that the name of LBLI should be used only in familial cases [7] and when an appearance similar to LBLI is observed in sporadic ALS cases, the name round inclusions would be better because the components of LBLI are different from those of LBLI-like inclusions. LBLI are indistinguishable from Lewy bodies seen in Parkinson's disease when stained with hematoxylin and eosin (H&E), but they are immunostained with Cu/Zu superoxide dismutase [12] but not -synuclein [1], while Lewy bodies are immunohistochemically positive for -synuclein [1]. Moreover, ALS with onset before the age of 20 has been reported as sporadic juvenile disease, in which cytoplasmic basophilic inclusions [4] have been observed as one of the characteristic features. Bunina bodies are immunohistochemically positive for cystatin C and ubiquitin-negative, while SLI and LBLI appear as

ubiquitin-positive, tau-negative, cystatin-C-negative, and -synuclein-negative. Basophilic inclusions show a globular or irregular-shaped appearance and are occasionally positive for ubiquitin with granular reaction. The mechanism for the formation of cytoplasmic inclusions remains unknown; therefore, elucidation of the main constituents is very important to understand the significance of these inclusions.

Transferrin, an 80-kDa glycoprotein, is an iron-binding plasma protein [2] that is capable of binding two iron atoms per molecule, diferric transferrin. Differing from monoferric transferrin and apotransferrin, diferric transferrin has a high affinity to transferrin receptor, a 180-kDa disulphide-bonded protein dimer of two identical subunits on the cell surface. Once iron-loaded transferrin binds to the transferrin receptor, the receptor–transferrin complex is internalized by endocytosis and the resulting endocytotic vesicle fuses with an acidic compartment. Dissociation of iron from transferrin occurs, and iron enters the cytoplasm. Apotransferrin is released extracellularly and binds more iron [10].

Neurons do not synthesize transferrin, although transferrin is synthesized within the oligodendrocytes [2] and choroid plexus epithelial cells of the third and lateral ventricles [3]. Therefore, plasma proteins like transferrin are thought to reach the neurons by endocytosis [10], the uptake of iron-loaded transferrin via transferrin receptor, or by nerve terminals at the area where the plasma proteins passage the nerve terminal from the blood and then retrograde transport occurs [11, 15, 26]. Large polygonal and pyramidal cells show more transferrin immunoreactivity in the amygdala and brainstem, reflecting the high densities of transferrin receptor on these cells [16]. Liu et al. [11] reported that 90–100% of neurons of the spinal cord as well as their axons of anterior horn cells show strong immunostaining for albumin and moderate to strong staining for transferrin.

Little attention has been paid to transferrin expression in neurodegenerative diseases. To better understand abnormal protein accumulation in the remaining anterior horn cells in ALS, we examined spinal cords from 12 ALS patients including two cases of ALS with dementia (ALS-D) and two cases of basophilic inclusion type of ALS, using antibodies against transferrin. We found that transferrin localized in Bunina bodies and some of the basophilic inclusions, in addition to diffuse cytoplasmic distribution of transferrin in the anterior horn cells.

Materials and methods

We examined a total of 12 ALS lumbar spinal cords (average patient age: 59.3 years old, sex: 6 males, 6 females) including two ALS-D cases (64-year-old female and 46-year-old male) and two ALS cases demonstrating basophilic inclusions (24- and 27-year-old females), in addition to samples from five non-ALS patients with Parkinson's disease, Alzheimer's disease, or Creutzfeldt–Jakob disease. Spinal cord tissues were all obtained from institutes and universities. In all cases, the autopsies were performed in accordance with established procedures and the samples were used in this study after obtaining informed consent from the family of each patient. All patients were definitively diagnosed based on clinical and light microscopic findings of the spinal cords and some of the data from several patients were previously reported elsewhere [4, 13]. Spinal cords were fixed with 4% paraformaldehyde in phosphate-buffered solution (PBS) (pH 7.4) and embedded in paraffin. Five micrometer thick transverse paraffin sections were prepared for immunohistochemistry, which was carried out using a rabbit polyclonal anti-human transferrin antibody (1:6,000; DakoCytomation, Glostrup, Denmark), a goat polyclonal anti-human transferrin antibody (1:20,000; MP Biomedicals, Ohio, USA), and rabbit polyclonal anti-albumin (1:5,000; DakoCytomation), anti-prealbumin (1:5,000; DakoCytomation), and anti-orosomucoid antibodies (1:2,000, DakoCytomation). For enhancement, autoclave treatment for 5 min was performed when anti-transferrin antibody was used. Sections were blocked in normal horse serum for 30 min at room temperature, then labeled with the first antibody at 4°C overnight, washed in PBS for 30 min, incubated with the second antibody provided by Histofine SAB-PO kit (Nichirei, Tokyo, Japan), washed in PBS for 30 min, and finally visualized by the avidin–biotin-peroxidase method. Observation was performed using an Olympus BX50 microscope.

Specificity of the transferrin staining was confirmed by preabsorption of the antibody for 1 h at 4°C with 100 M human transferrin (Sigma).

For Bunina bodies, Lewy body-like inclusions, and basophilic inclusions, H&E staining was initially performed to observe the locations of these structures. After photographing these findings, were moved the cover glasses from the slides in xylene, decolorized the specimens in alcohol, and performed the same process for transferrin immunostaining.

Results

In general, the cytoplasm and processes of the anterior horn cells showed almost homogeneously transferrin-positive immunoreactivities in ALS and non-ALS

cases (Fig. 1), although the intensities differed in each anterior horn cell, ranging from weak staining to strong staining. In addition, small cells were seen between and around the anterior horn cells, in which transferrin-positive products were detected adjacent to the nuclei (arrows in Fig. 1). Transferrin immunoreactivity was confined to a thin rim of perinuclear cytoplasm in a cap-like fashion, suggesting that these cells were oligodendrocytes (data not shown), as previously reported [2]. Little differences of transferrin immunoreactivity among each anterior horn cell were seen in ALS, ALS-D, the basophilic type of ALS, and non-ALS cases.

In addition to weak staining of transferrin within the cytoplasm, small transferrin-positive circular structures were observed in the cytoplasm of anterior horn cells in all ALS cases except one sporadic case (Fig. 2a). The periphery of their structures showed strong immunoreactivity compared to that at the center. The number of transferrin-positive structures varied in each spinal cord section. To determine whether the transferrin-positive reactions were specific, a serial section was immunostained after preabsorption of anti-transferrin antibody with human transferrin for 1 h at 4° C. The finding showed that transferrin-positive staining disappeared (Fig. 2b), indicating that the reaction was true.

Since circular transferrin-positive staining likely corresponded to Bunina bodies, H&E staining was performed initially to confirm where those structures showing eosinophilic inclusions were located (Fig. 3a, c). After photographing the Bunina bodies shown by H&E staining, immunohistochemistry for transferrin was examined on the same section. The results showed that transferrin immunoreactivies (Fig. 3b, d) were seen at the same location as Bunina bodies, indicating that transferrin was co-localized with Bunina bodies and that Bunina bodies were related to transferrin. Using a different anti-human transferrin antibody purchased from MP Biomedicals, Bunina bodies were similarly shown as transferrin positive (data not shown). Bunina bodies were not immunoreactive for other plasma proteins such as albumin, prealbumin, and orosomucoid (data not shown).

Lewy body-like inclusions or round inclusions showing an eosinophilic core with a peripheral halo appearance were detected on H&E staining in a sporadic ALS case (Fig. 4a, c). After the H&E stained section was decolorized by alcohol, transferrin staining was performed, showing a slightly stronger immunoreaction for Lewy body-like inclusions at the core than in the cytoplasm (Fig. 4b, d). However, the staining level was obviously weak compared to that of Bunina bodies.

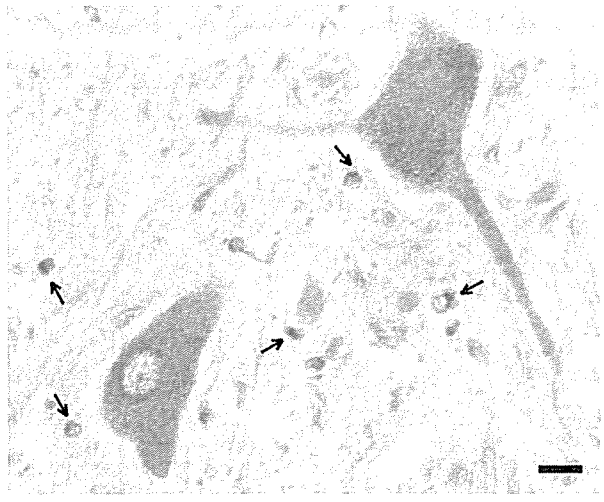

Fig. 1 Transferrin immunoreactivitiy in anterior horn cells. Cytoplasm and processes were diffusely transferrin positive. Small cells showing transferrin-positive immunoreactivity were scattered around the anterior horn cells (*arrows*). Scale bar: 20 m

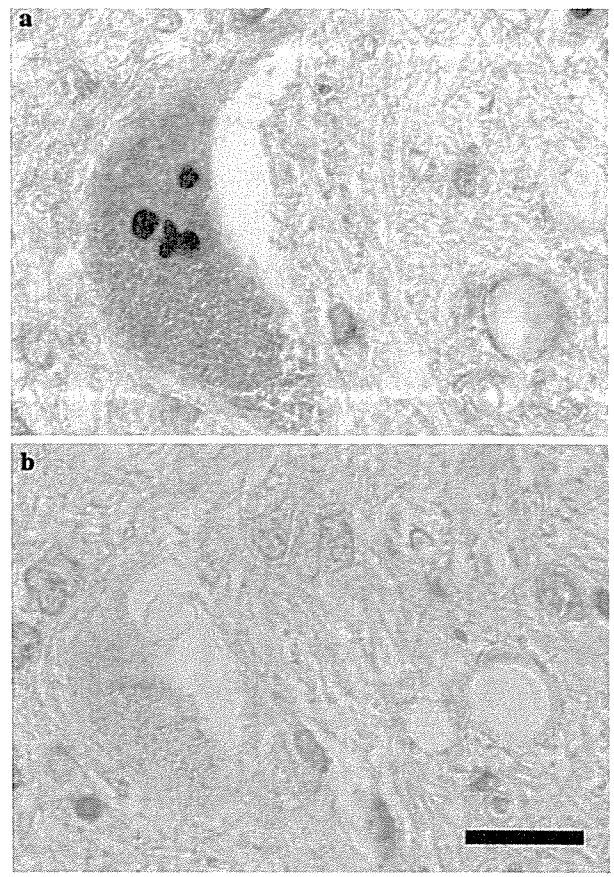

Fig. 2 Transferrin immunoreactivitiy in small circular structures. **a** Immunostaining for transferrin. **b** Immunostaining for transferrin preabsorbed with human transferrin. Transferrin immunostaining was obviously specific. Scale bar: 20 m

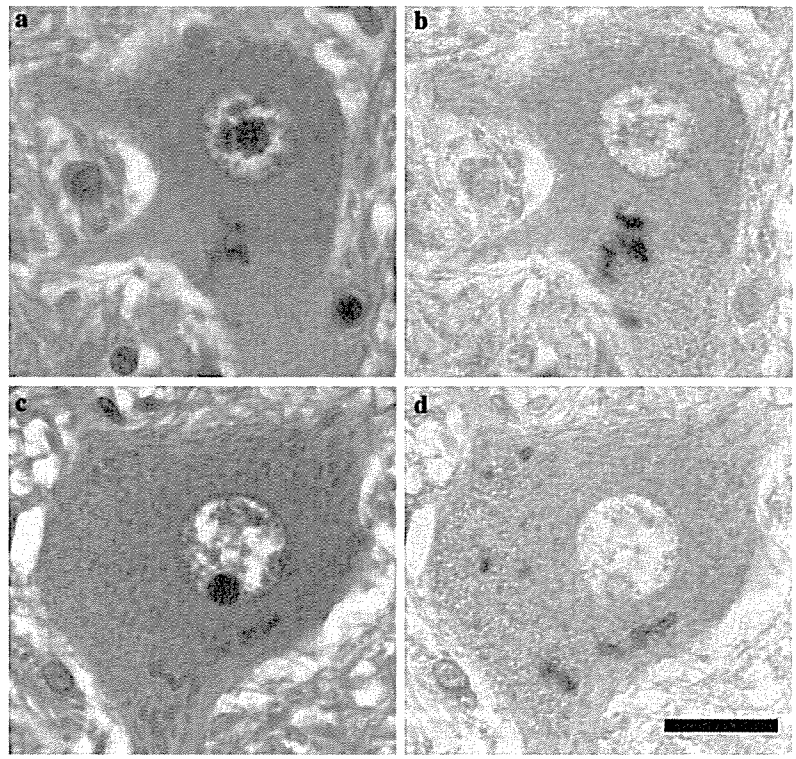

Fig. 3 Transferrin immunoreactivity in Bunina bodies. **a**, **c** H&E staining. **b**, **d** Immunostaining for transferrin. Bunina bodies (**a**, **c**) were transferrin positive. The presence of Bunina bodies was confirmed with H&E staining (**a**, **c**), and the same section was examined with anti-transferrin antibody (**b**, **d**). Scale bar: 20 m

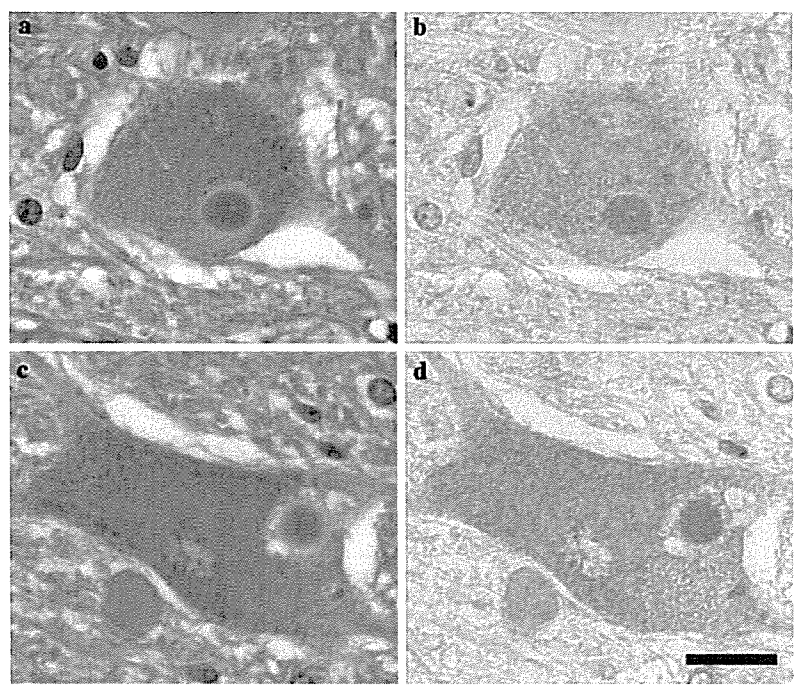

Fig. 4 Transferrin immunoreactivity for Lewy body-like inclusions. **a**, **c** H&E staining. **b**, **d** Immunostaining for transferrin. The presence of Lewy body-like inclusions was confirmed with H&E staining (**a**, **c**), and the same section was examined with anti-transferrin antibody (**b**, **d**). Scale bar: 20 m

Confirming t he horseshoe-shaped, m ultilobulated, globular, tubular or spheroid inclusions that appeared basophilic in t he cy toplasm of a nterior hor n ce lls on H&E s taining, which we re r ecognized a s basophilic inclusions (B I), (Fig. 5a, c, e, g), we ex amined 1 5 B I detected in t wo A LS ca ses to de termine wh ether the structures w ere p ositive fo r tr ansferrin. T he findings demonstrated that immunoreactive pa tterns for tr ansferrin we re ro ughly cla ssified into th ree typ es. Fi ve obvious tr ansferrin-positive B I w ere de tected am ong

15 inclusions (Fig. 5b, d), although the immunoreactivity was h eterogeneous not h omogeneous. Furthermore, detectable but weak heterogeneous immunostaining was observed in five inclusions (Fig. 5f). There were five BI that were almost transferrin negative (Fig. 5h).

We ob served num erous ske in-like in clusions show-ing p 62-positive staining o f sections fr om ALS cases, however, these in clusions were t ransferrin ne gative in the a djacent s ections (data not s hown). F urthermore, other structures such as granulovacuolar degeneration and neurofibrillary tangles in Alzheimer's disease were not immunostained for transferrin (data not shown).

Discussion

Among comparatively A LS-specific s tructures such as Bunina bodies [21, 23], skein-like in clusions [9], Lewy body-like inclusions or rou nd inclu sions [6, 7, 14] an d basophilic inclu sions [4], Bu nina bo dies sh owed ob vi-ous immunoreactivity fo r transferrin. Th e or igin of Bunina bo dies i s u nknown, h owever, s everal a uthors have reported that it co uld be re lated t o a utophagic vacuole [5] and Golgi apparatus [19, 22]. Recently, we found that skein-like inclu sions, LBLI or r ound inclu-sions, and so me of t he b asophilic in clusions in the remaining anterior ho rn ce lls we re p6 2 positive [13], while Bunina bodies were negative for p62. These find-ings are interesting because skein-like inclusions, LBLI or round in clusions, a nd some of the b asophilic inclu-sions are immunoreactive for ubiquitin.

Cystatin C is a member of a super family of protease inhibitors, a nd i nvolved in p rocesses su ch a s t umor invasion a nd m etastasis, in flammatory pro cesses, a nd some ne urological di seases [25]. Ok amoto e t al. [23] reported t hat cy statin C loca lizes in B unina bo dies o f ALS c ases. I n addition t o the increase o f 1 4-3-3 pro-teins in t he cerebrospinal fluid (CSF), cystatin C could also be one of t he i nteresting d iagnostic m arkers o f sporadic Cr eutzfeldt–Jakob dis ease [24]. I n c ontrast, cystatin C in the CSF has been found to be down-regu-lated in pa tients with le ptomeningeal metastasis [18], Guillain–Barre sy ndrome [17], or chro nic in flamma-tory demyelinating polyneuropathy [17]. Transferrin is a m ajor glycoprotein playing an important role in the transport o f cir culating f erric ir on a nd i ts de livery t o tissues th at ex press surface tr ansferrin re ceptor. T he presence of un usual glycosylated isoforms of transfer-rin and the specific enrichment and oxidation of trans-ferrin i soforms ha s b een re ported in Al zheimer's disease (AD) plasma [29]. Moreover, Piubelli et al. [24] demonstrated t hat transferrin is fivefold up-regulated

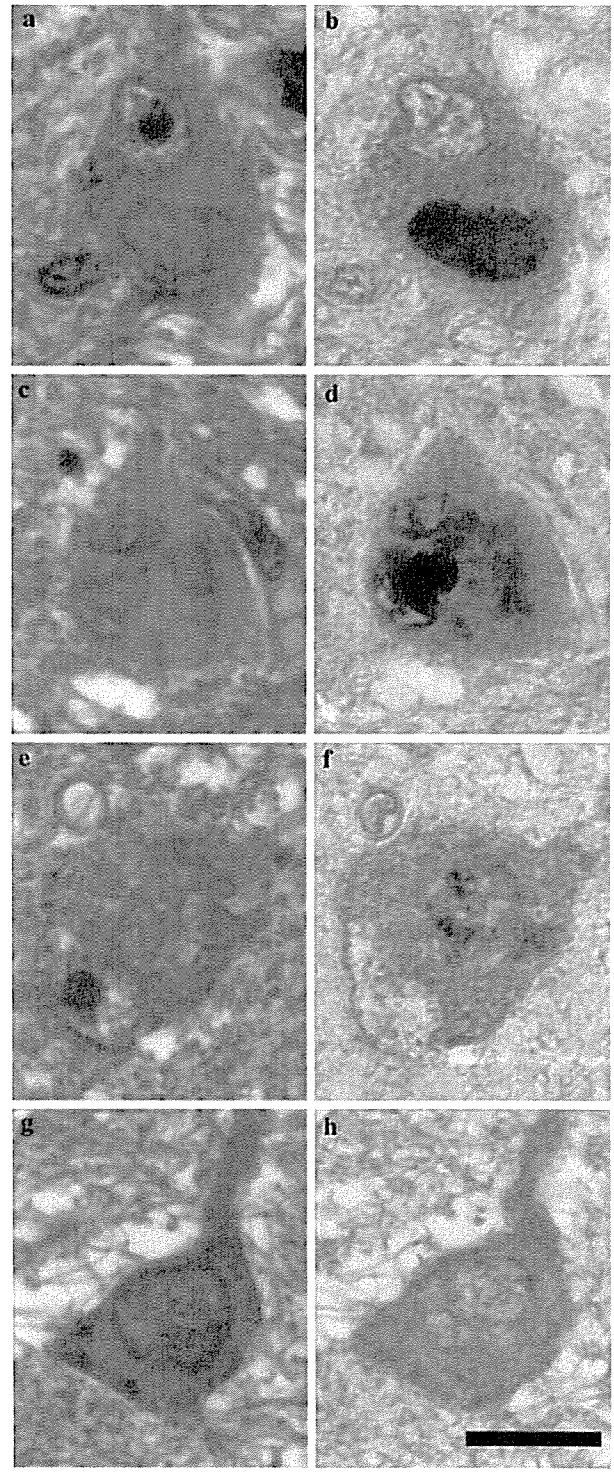

Fig. 5 Transferrin immunoreactivity for bas ophilic inclusions. **a, c, e, g** H&E staining. **b, d, f, h** Immunostaining for transferrin. Basophilic i nclusions s howed str ongly t ransferrin-positive (**b, d**), w eak (**f**) and neg ative (**h**) re action. The presence of th ese structures was confirmed with H&E on same sections. Scale bar: 20 m